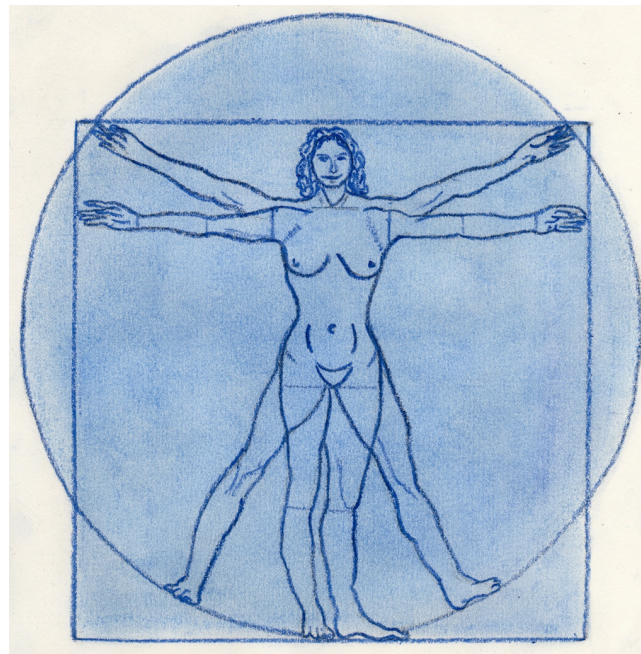


Серийные, сетевые и глубинные маркеры (и немного про генетический интеллект)



Проф Алексей Заикин

Institute for Women's Health and Department of Mathematics
University College London

www.zaikinlab.com

alexey.zaikin@ucl.ac.uk



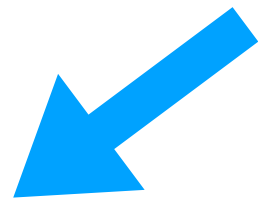
ЦАСС
Центр анализа
сложных систем



СЕЧЕНОВСКИЙ
УНИВЕРСИТЕТ



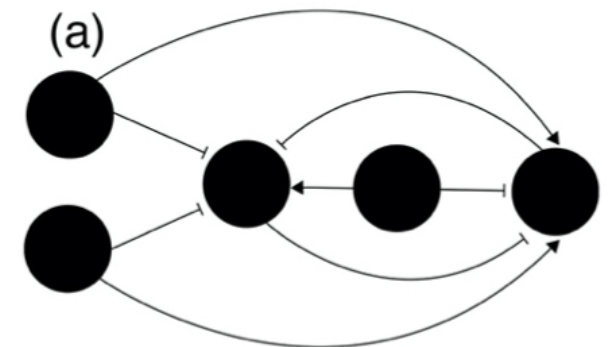
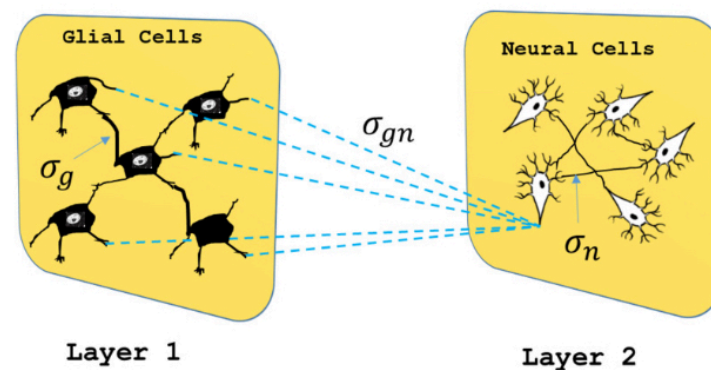
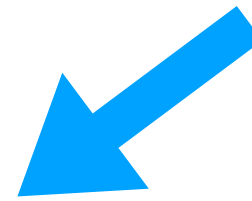
www.zaikinlab.com



Data analysis

Зам глав врача: искусственный интеллект пока приносит лечащему врачу больше хлопот чем пользы

Mathematical modelling



Content and aim: review of possible collaborations

Data analysis:

Longitudinal analysis

Proteome

Network analysis

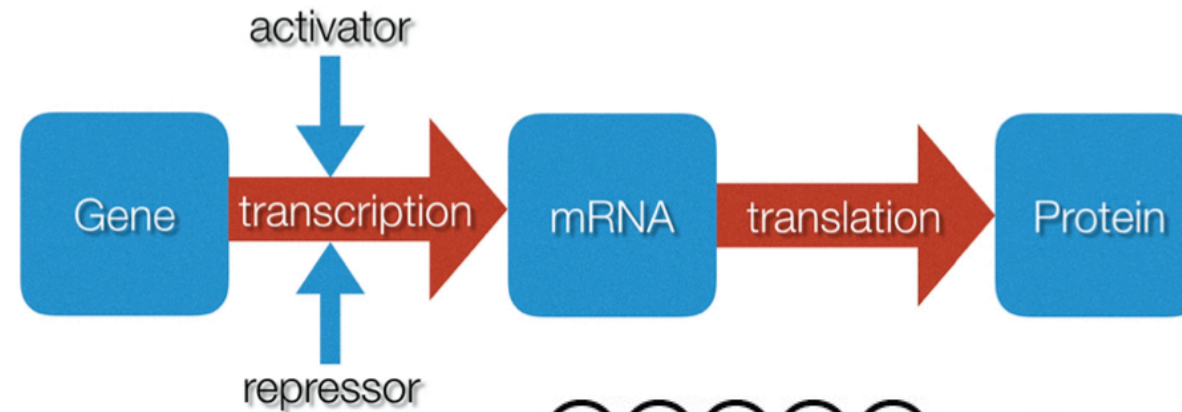
Epigenome

Deep learning analysis

Images

Transcriptional regulation

- Basic paradigm of molecular biology. Kind of a "Newton's law" for living systems:



Omic
Information:
Small
review on
molecular
biology

Epigenetics and MicroRNAs

JODY C. CHUANG, AND PETER A. JONES

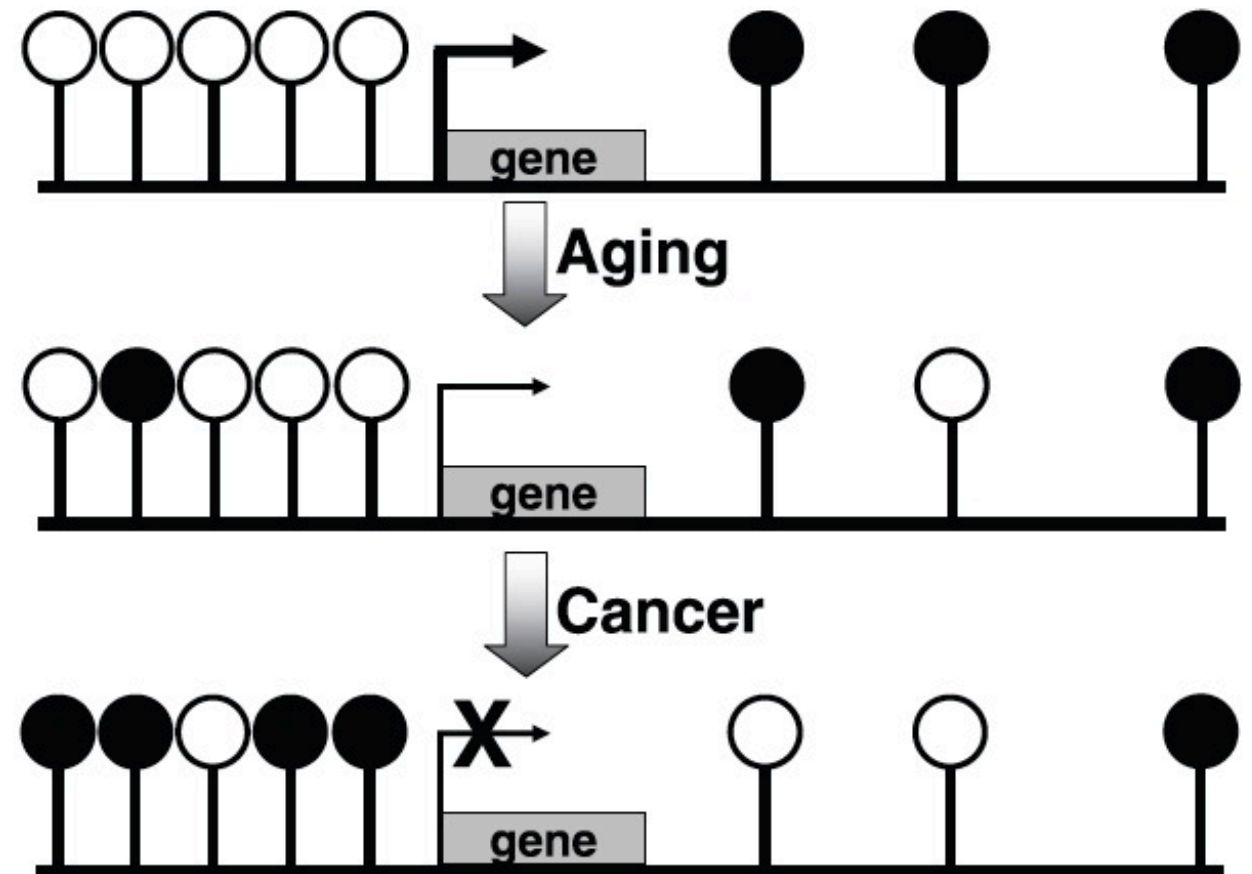


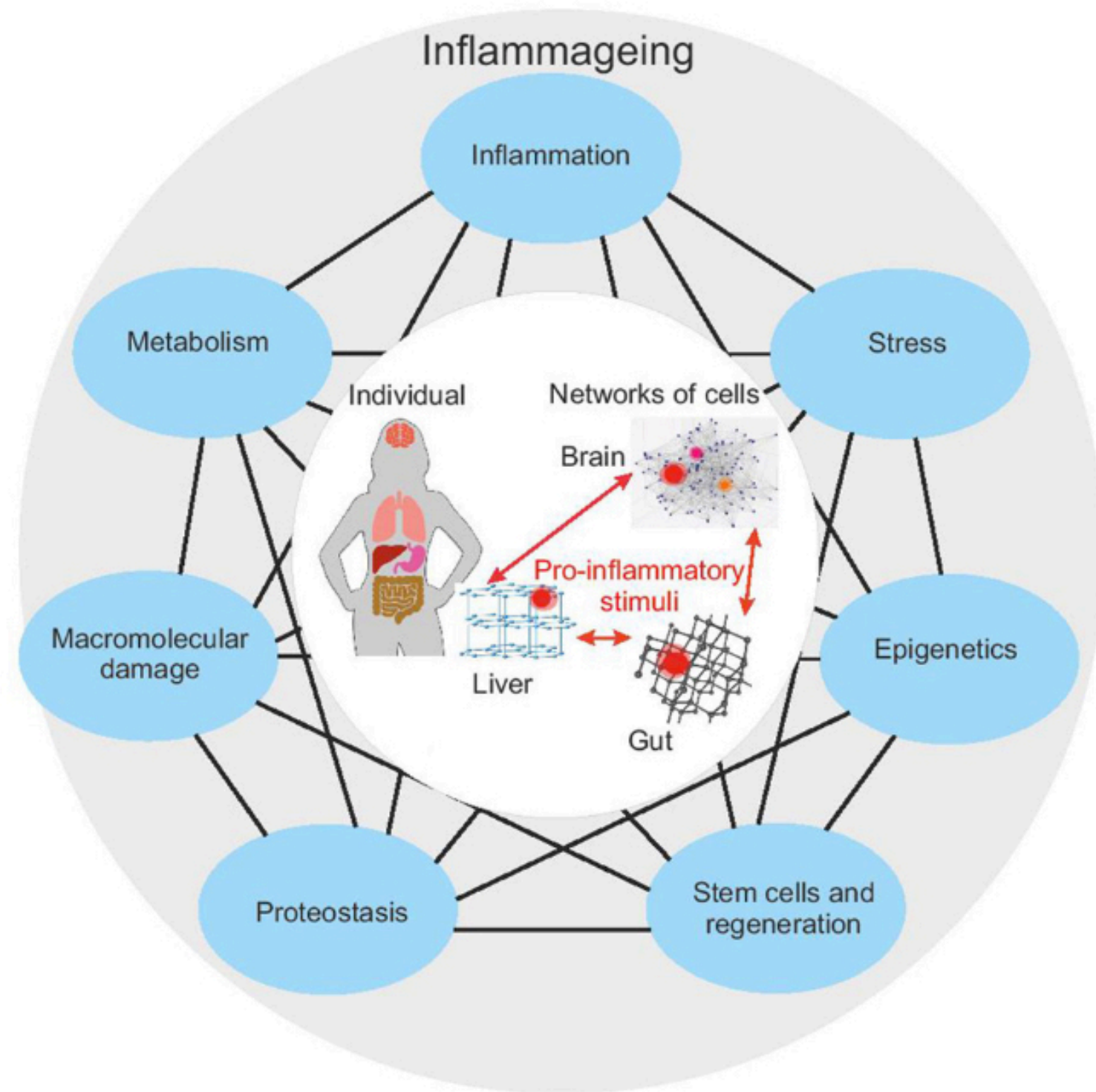
Figure 3. CpG islands normally remain unmethylated, whereas the sporadic CpG sites located in the rest of the genome often are methylated. With aging, there is a gradual reversal of this phenomenon. During carcinogenesis, this change is much more dramatic, leading to a global hypomethylation and hypermethylation of CpG islands. The results are chromosomal instability and silencing of some important tumor-suppressor genes.

Personalised medicine



The Human Body as a Super Network: Digital Methods to Analyze the Propagation of Aging

Harry J. Whitwell¹, Maria Giulia Bacalini², Oleg Blyuss^{3,4}, Shangbin Chen⁵, Paolo Garagnani⁶, Susan Yu Gordleeva⁷, Sarika Jalan^{8,9}, Mikhail Ivanchenko¹⁰, Oleg Kanakov⁷, Valentina Kustikova¹⁰, Ines P. Mariño¹¹, Iosif Meyerov¹⁰, Ekkehard Ullner¹², Claudio Franceschi^{7,10*} and Alexey Zaikin^{4,10,13*}



V. Samborska et al. MAMMALIAN BRAIN AS A NETWORK...

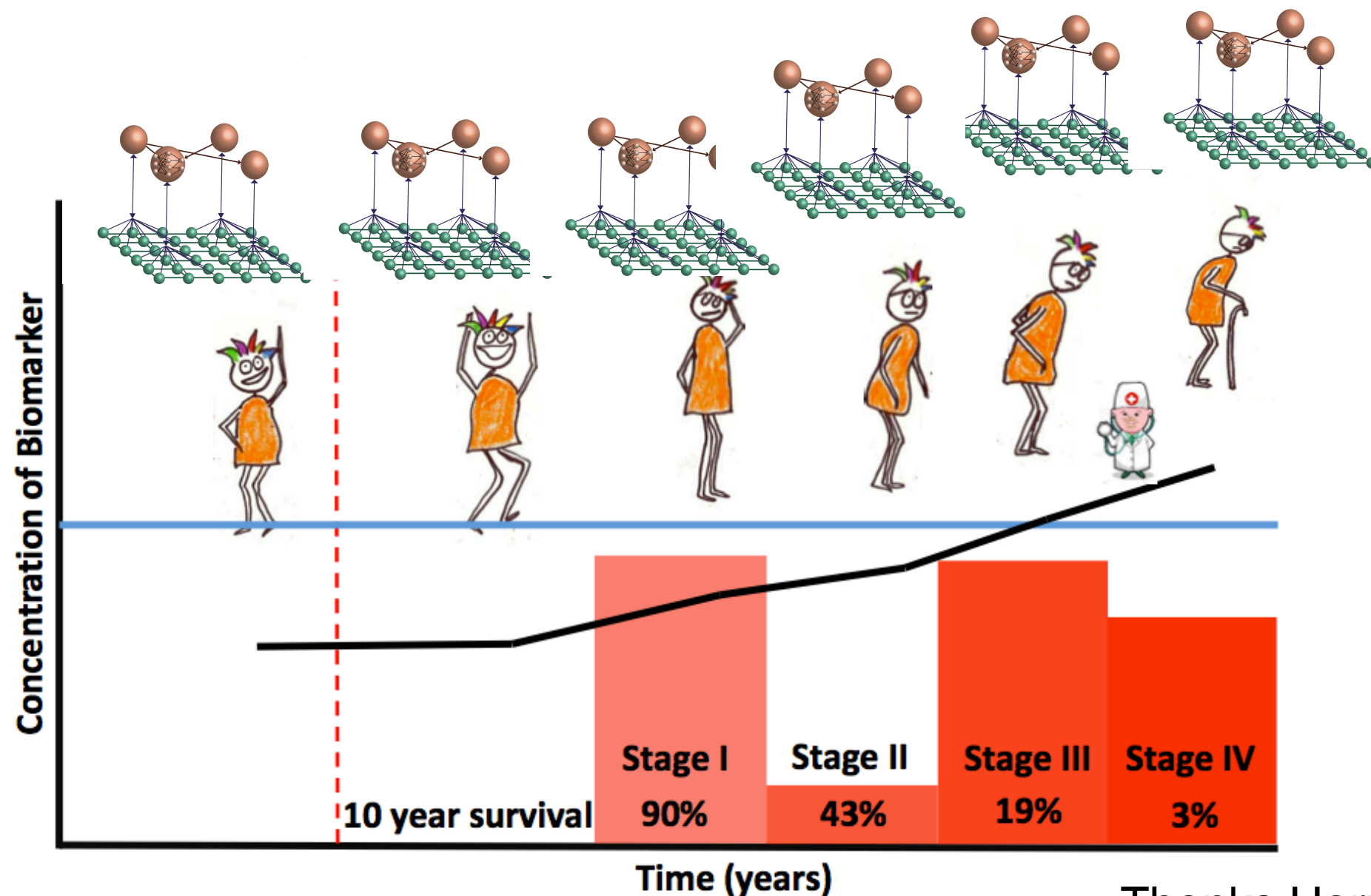
OM&P

MAMMALIAN BRAIN AS A NETWORK OF NETWORKS

Veronika Samborska¹, Susanna Gordleeva², Ekkehard Ullner³, Albina Lebedeva², Viktor Kazantsev², Mikhail Ivanchenko² and Alexey Zaikin^{2,4}

Search for Network, Longitudinal and Deep Learning Biomarkers

Multi-omic data: Genetic, Epigenetic and Proteomic



Thanks Harry for picture

Longitudinal and deep learning markers

a First-Line Screen for Ovarian Cancer

- Ovarian cancer remains the leading cause of death from gynecological cancer among women and accounts for 5% of all female deaths from cancer, corresponding to **annual deaths of around 4,100 in the United Kingdom, 42,700 in Europe, 22,280 in the United States and 152,000 worldwide.**
- Most women are diagnosed in advanced stage (Stage III–IV) with reported **5-year survival rates of 19% (Stage III) and 3% (Stage IV)** respectively. The **higher survival rates of 70%–90% in earlier stage (Stage I–II)** disease has driven international screening efforts to detect the disease earlier.
- In **the United Kingdom Collaborative Trial of Ovarian Cancer Screening (UKCTOCS)**, women in the multimodal (MMS) arm had a serum CA125 test (first-line), with those at increased risk, having repeat CA125/ultrasound (second-line test). CA125 was interpreted using the "Risk of Ovarian Cancer Algorithm" (ROCA).
- Experimental Design: **50,083 post-menopausal women** who attended 346,806 MMS screens were randomly split into training and validation sets, following stratification into cases (ovarian/tubal/peritoneal cancers) and controls.

Markov Chain Monte-Carlo Approximate Bayesian Computation and Bayesian Change Point Models

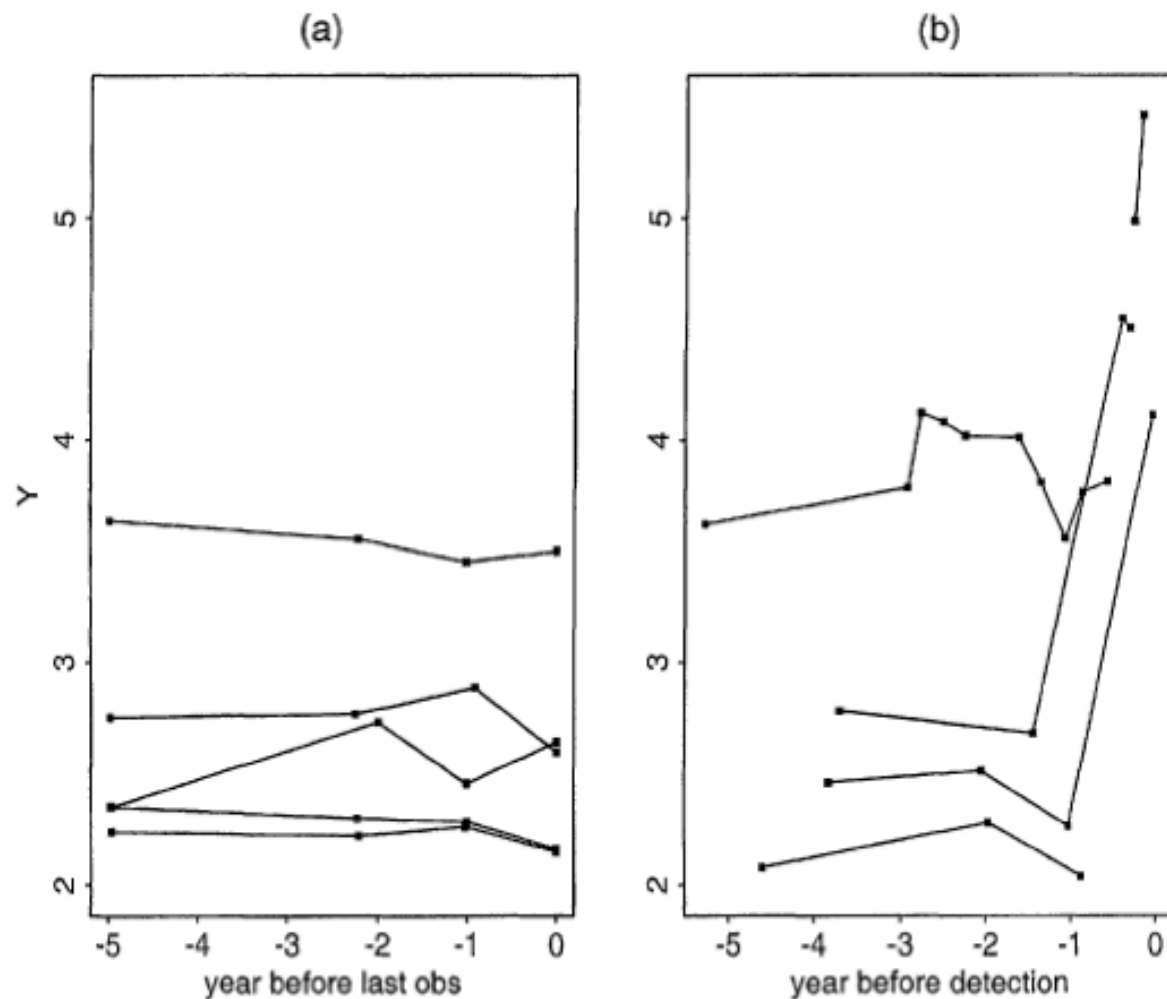
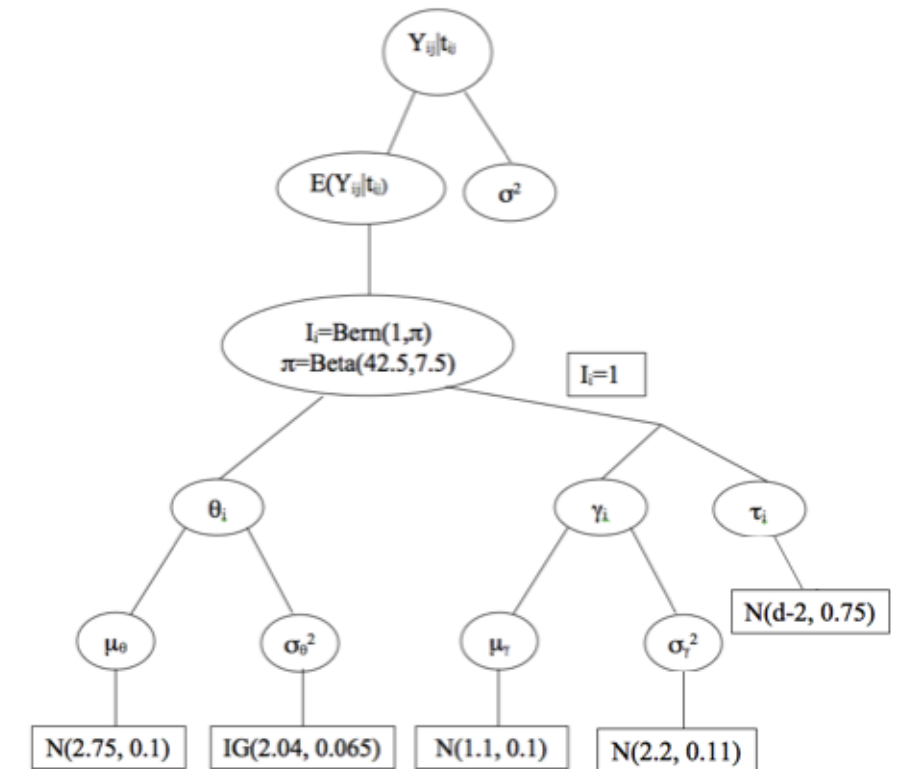
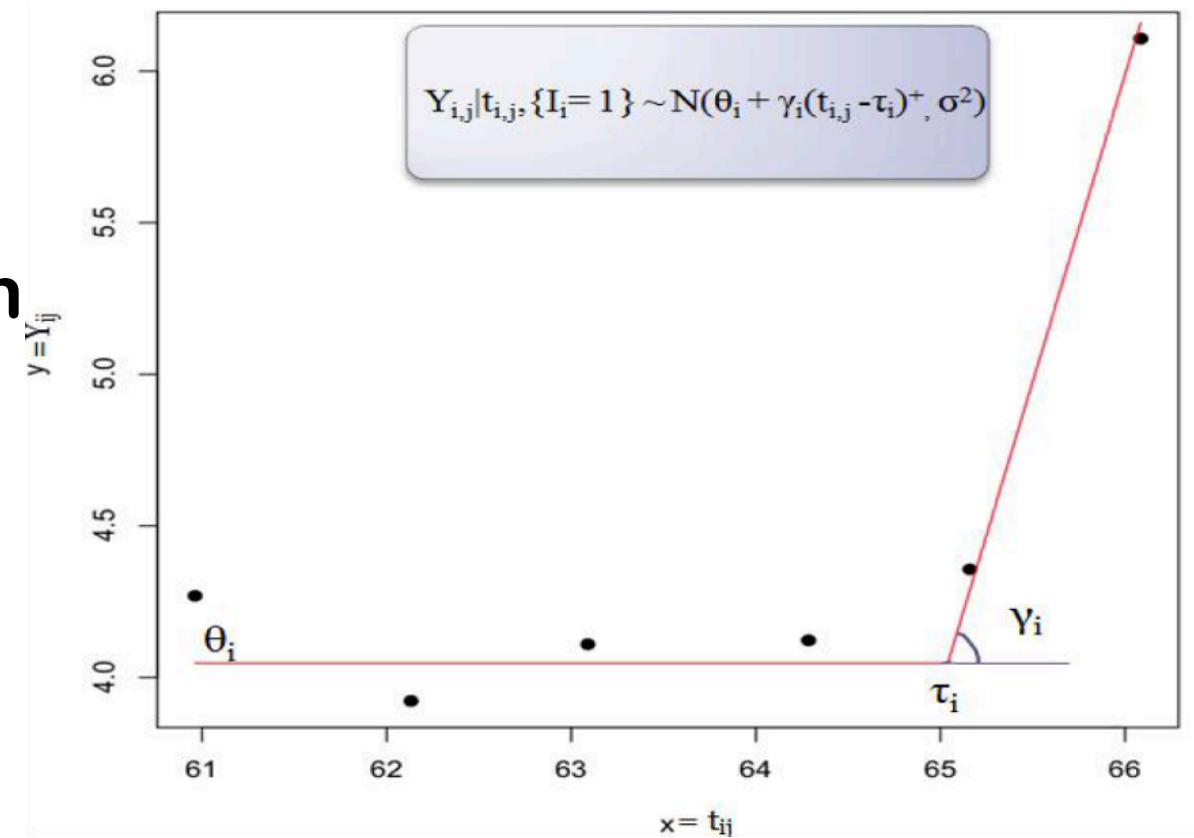


Figure 1. Transformed CA125 Values (Y) From Five Controls (a) and Five Cases (b) in the U.K. Screening Trial (Jacobs et al. 1993).

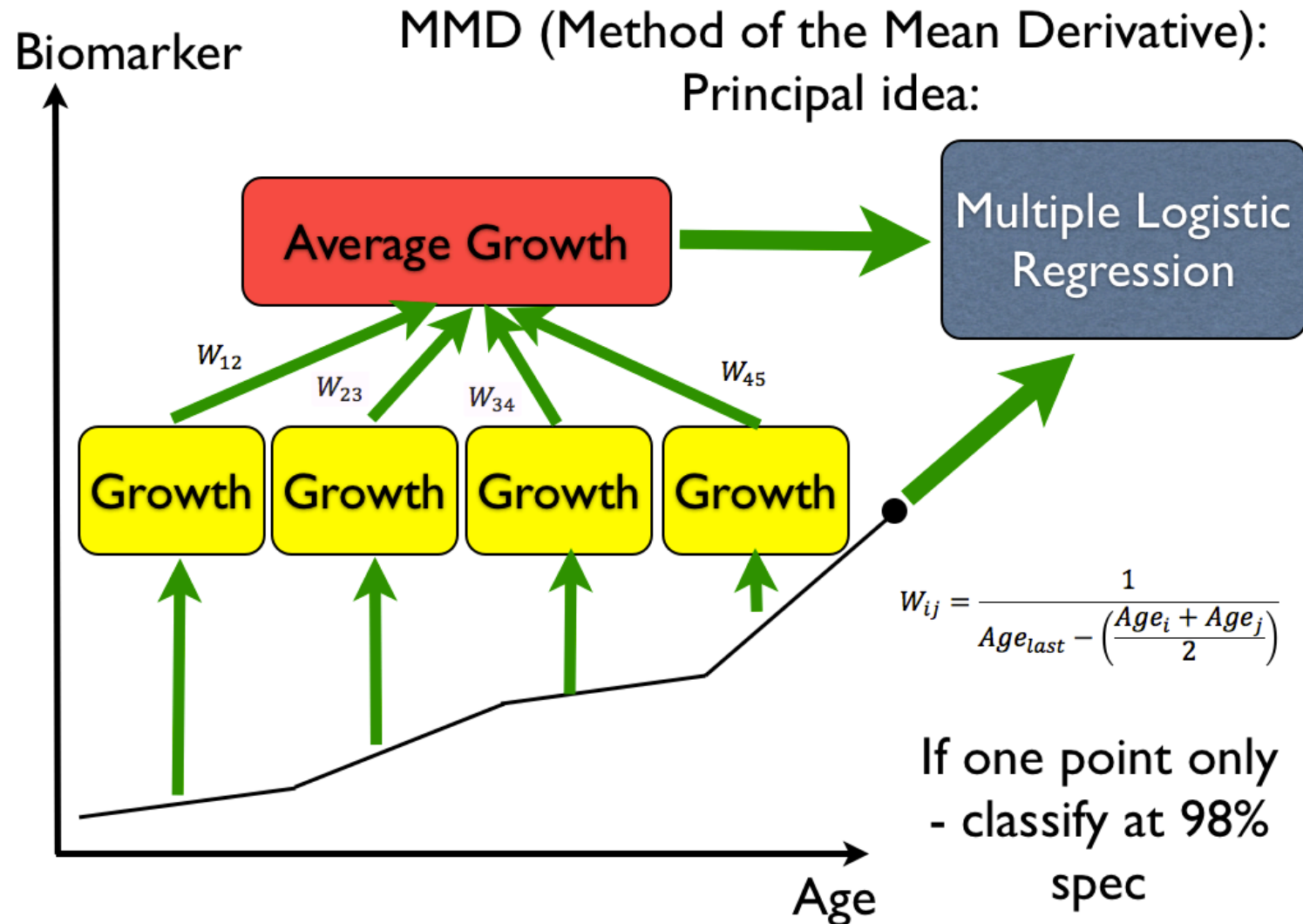


Change-point of multiple biomarkers in women with ovarian cancer



Inés P. Mariño^{a,b,*,1}, Oleg Blyuss^{b,1}, Andy Ryan^b, Aleksandra Gentry-Maharaj^b, John F. Timms^b, Anne Dawnay^c, Jatinderpal Kalsi^b, Ian Jacobs^{b,d}, Usha Menon^{b,2}, Alexey Zaikin^{b,2}

Method of Mean Trends



Comparison of longitudinal CA125 algorithms as a first line screen for ovarian cancer in the general population

Oleg Blyuss¹, Matthew Burnell¹, Andy Ryan¹, Aleksandra Gentry-Maharaj¹, Inés P. Mariño^{1,2}, Jatinderpal Kalsi¹, Ranjit Manchanda^{1,6}, John F. Timms¹, Mahesh Parmar³, Steven J. Skates⁴, Ian Jacobs^{1,5,8}, Alexey Zaikin^{1,7*}, and Usha Menon^{1*}.

Indicators used (for every i -th patient):

- Last measurement
- Trend 1 (Mean derivative)

$$\left(\sum_{j=1}^{k_i-1} \frac{y_{j+1} - y_j}{t_{j+1} - t_j} \frac{1}{t_{k_i} - (t_{j+1} + t_j)/2} \right) / (k_i - 1)$$

- Trend 2

$$\left(\sum_{j=1}^{k_i-1} \frac{(y_{j+1} - y_j)(t_{j+1} - t_j)}{2} \right) / (k_i - 1)$$

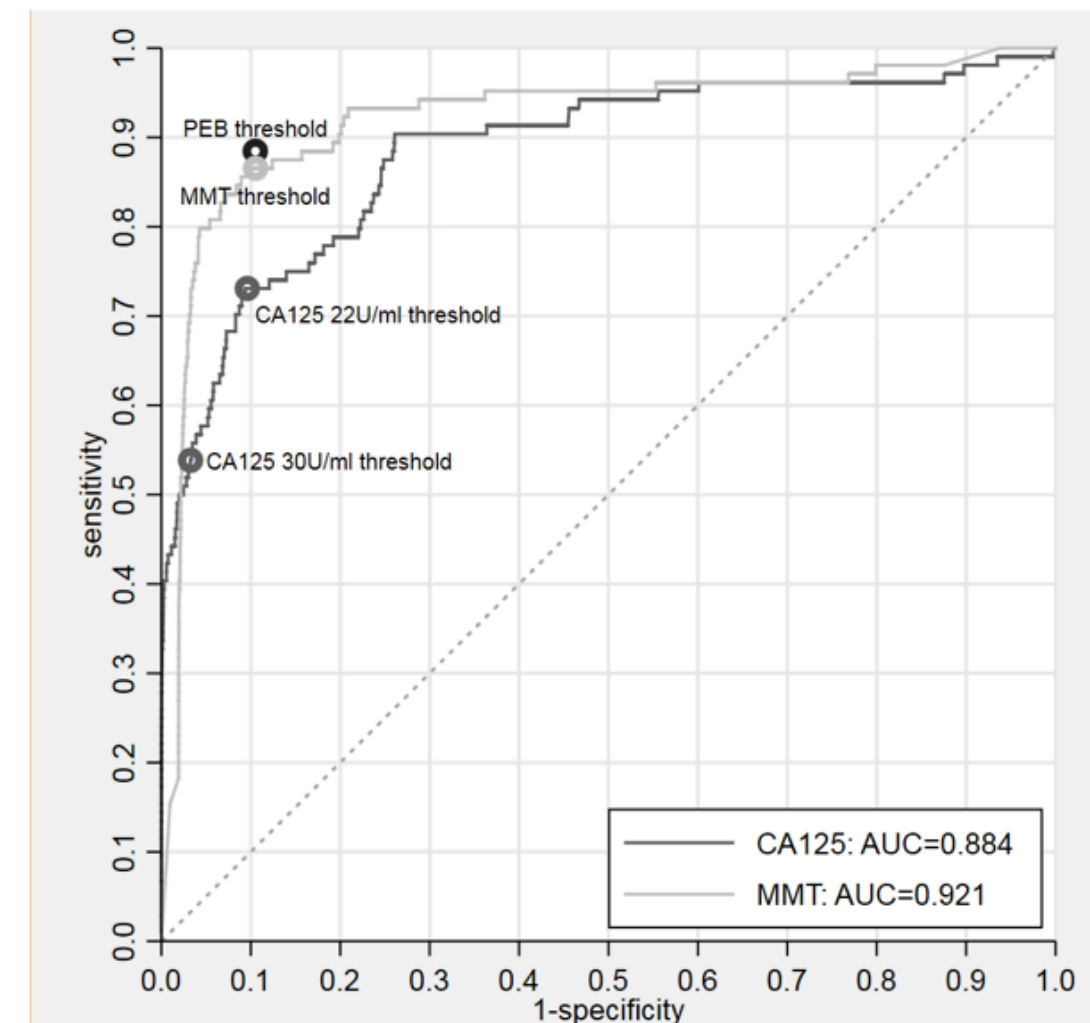
- Trend 3

$$\sqrt{\frac{\sum_{j=1}^{k_i} (y_j - \bar{y})^2}{k_i}} / \bar{y}$$

- Trend 4

$$\frac{\sum_{j=1}^{k_i} y_j t_j}{\sum_{j=1}^{k_i} t_j}$$

- Trend 5 (Variance)



- Key papers:
- finding longitudinal oncomarkers- **License obtained!**

Published OnlineFirst July 3, 2018; DOI: 10.1158/1078-0432.CCR-18-0208

Precision Medicine and Imaging

Clinical
Cancer
Research

Comparison of Longitudinal CA125 Algorithms as a First-Line Screen for Ovarian Cancer in the General Population

Oleg Blyuss¹, Matthew Burnell¹, Andy Ryan¹, Aleksandra Gentry-Maharaj¹, Inés P. Mariño^{1,2}, Jatinderpal Kalsi¹, Ranjit Manchanda^{1,3}, John F. Timms¹, Mahesh Parmar⁴, Steven J. Skates⁵, Ian Jacobs^{1,6,7}, Alexey Zaikin^{1,8}, and Usha Menon¹

4726 Clin Cancer Res; 24(19) October 1, 2018

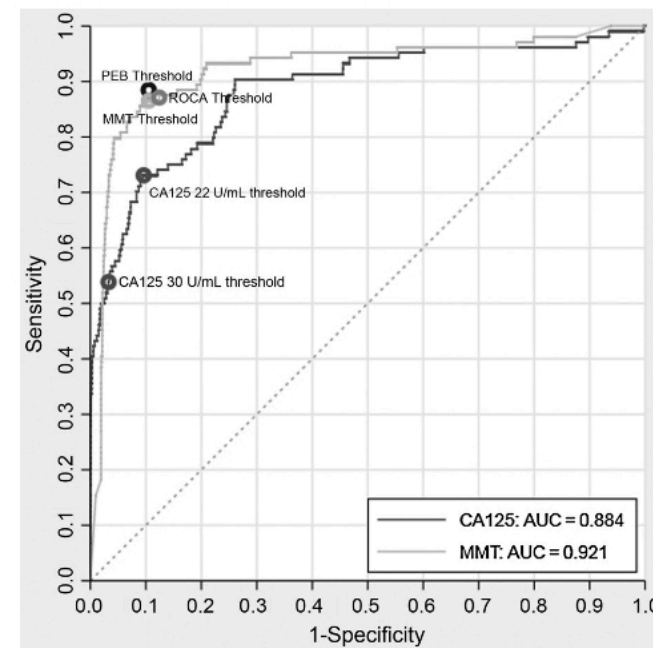


Figure 1.

Performance characteristics of CA125 interpreted using MMT, threshold rules, PEB and ROCA for detection of iEOC/PPC cases. Circle points give particular values of sensitivity and specificity provided by MMT and PEB corresponding to cutoff values obtained from the training set (MMT and PEB), CA125 using 22 and 30 U/mL cutoff values and ROCA as reported in ref. (6). Abbreviations: PEB, parametric empirical Bayes; MMT, method of mean trends; CA125, cancer antigen 125; AUC, area under roc-curve.

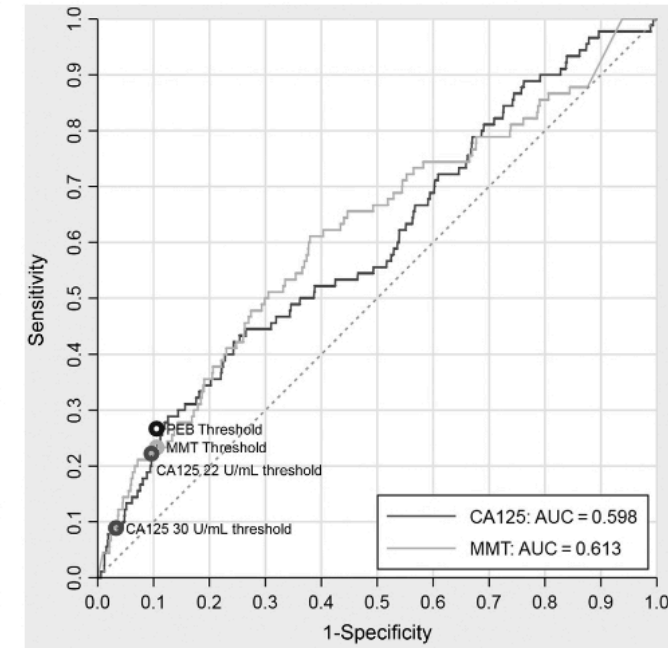


Figure 2.

Secondary analysis ROC curves for CA125 interpreted using MMT, threshold rules and PEB for detection of iEOC/PPC cases. Circle points on the ROC curves give particular values of sensitivity and specificity provided by MMT and PEB corresponding to cutoff values obtained from the training set (MMT and PEB). Abbreviations: PEB, parametric empirical Bayes; MMT, method of mean trends; CA125, cancer antigen 125; AUC, area under roc-curve.

A quantitative performance study of two automatic methods for the diagnosis of ovarian cancer

Manuel A. Vázquez^{a,b,1}, Inés P. Mariño^{c,d,*,1}, Oleg Blyuss^{e,d}, Andy Ryan^d, Aleksandra Gentry-Maharaj^d, Jatinderpal Kalsi^d, Ranjit Manchanda^{d,f}, Ian Jacobs^{d,g,h}, Usha Menon^{d,2}, Alexey Zaikin^{d,i,j,2}

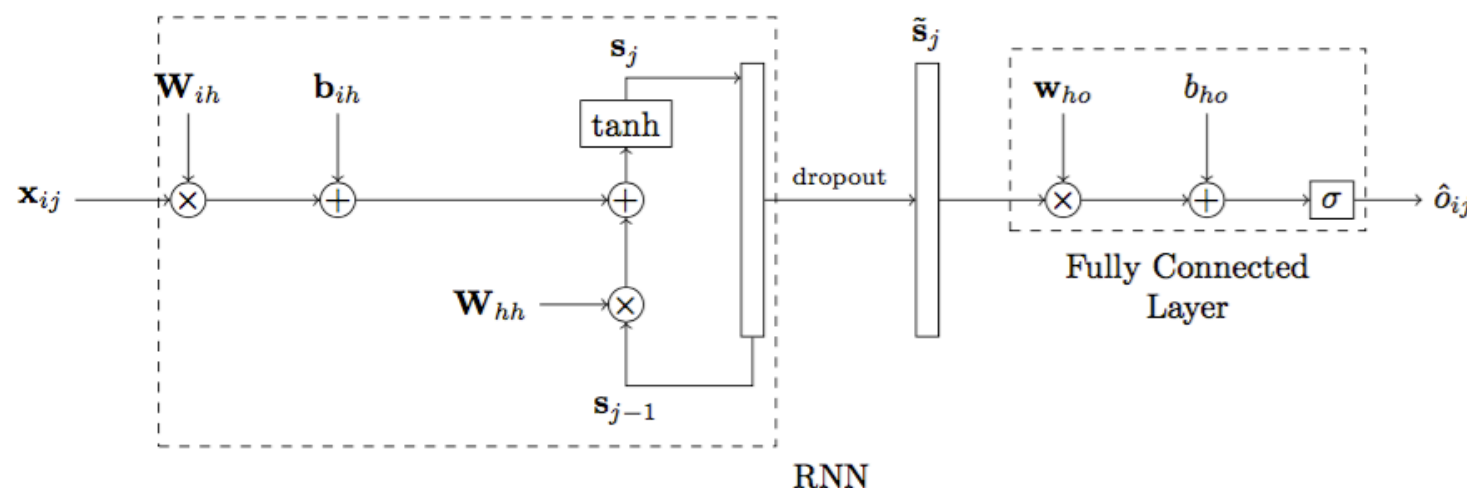
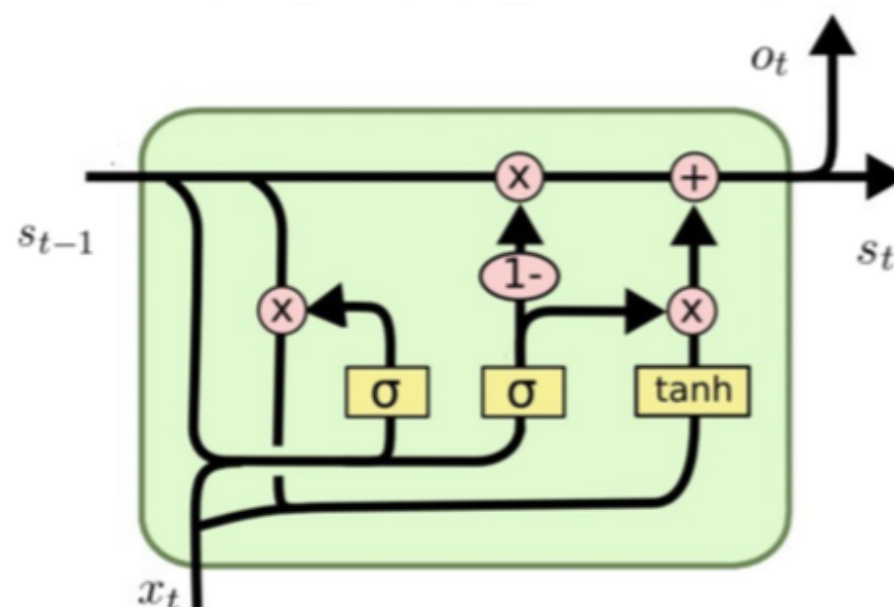


Fig 2. Network architecture for a single biomarker.

Development of neural network architecture for the early diagnosis analysis of oncomarker data in womens cancer

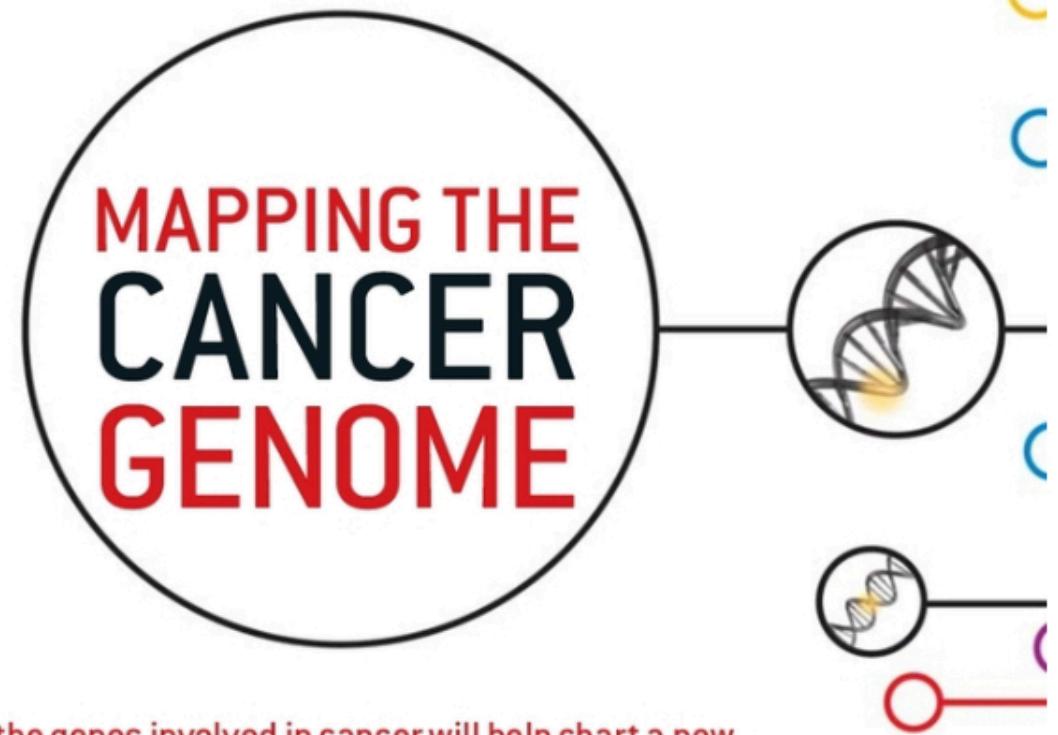


V. Cherepanova et al.

Work in progress!

Network markers

Constructing network biomarkers



Scientific American
Vol. 296, No. 3 (MARCH 2007), pp. 50-57 (8 pages)

Pinpointing the genes involved in cancer will help chart a new course across the complex landscape of human malignancies

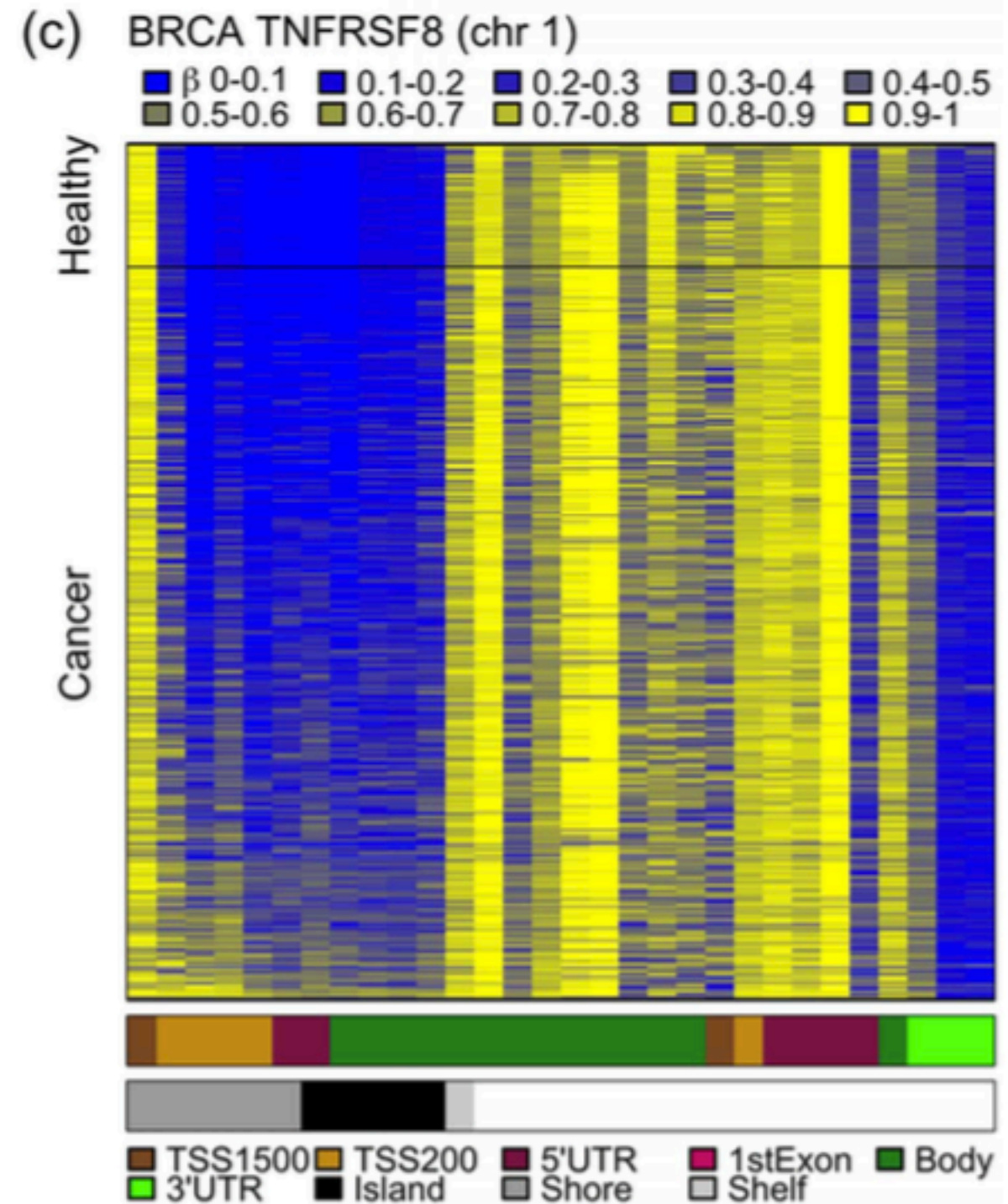
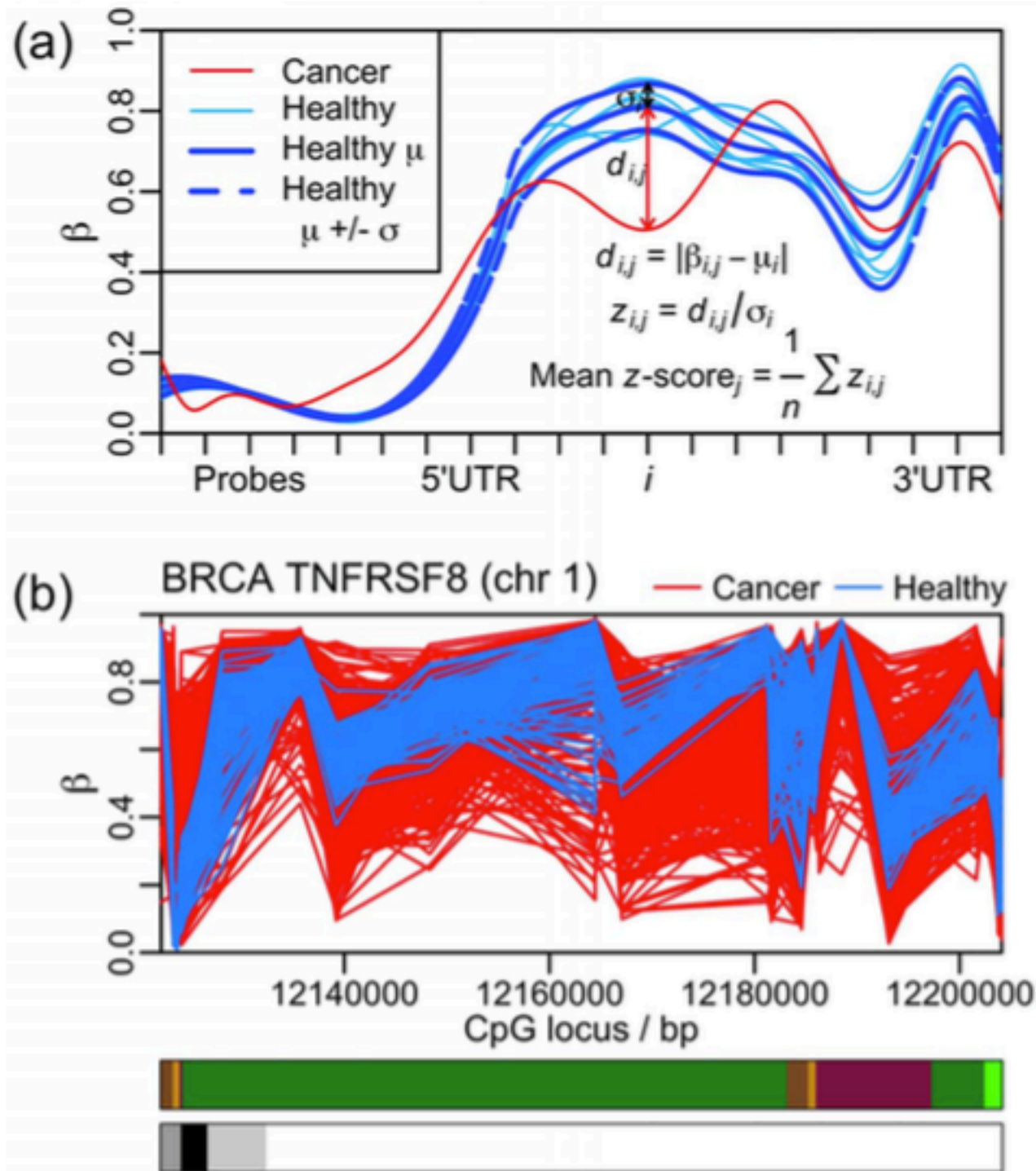
By Francis S. Collins and Anna D. Barker

*“One difficulty in interpreting this data for defining clinically useful information is that **multiple different changes** may be responsible for the onset of a disease, as exemplified by the efforts of The Cancer Genome Atlas project”*

- Network biomarkers for methylation: using correlations between intra-gene profiles
- Parenclitcal networks: constructing networks when links are unknown

Corruption of the Intra-Gene DNA Methylation Architecture Is a Hallmark of Cancer

Thomas E. Bartlett^{1,2}, Alexey Zaikin², Sofia C. Olhede^{1,3}, James West^{1,4}, Andrew E. Teschendorff⁴, Martin Widschwendter^{5*}



A DNA Methylation Network Interaction Measure, and Detection of Network Oncomarkers

Thomas E. Bartlett^{1,3*}, Sofia C. Olhede^{2,3}, Alexey Zaikin¹

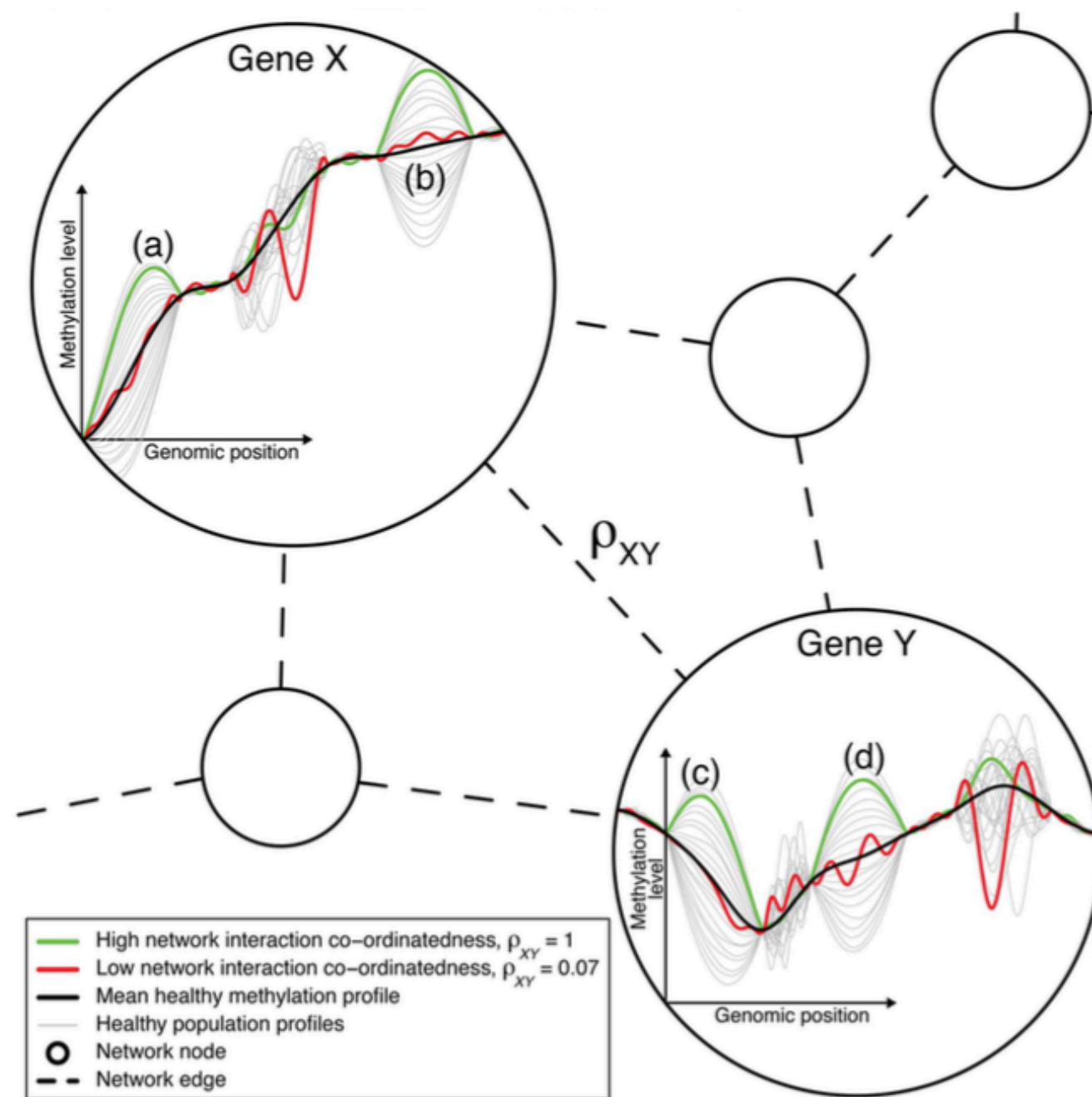


Figure 1. The DNA methylation network interaction measure. A combination of the variation of the healthy methylation profiles in regions (a) and (b) of gene X explains well/is well-explained by a combination of the variation of the healthy methylation profiles in regions (c) and (d) of gene Y. The green cancer sample varies by a large amount about the mean methylation profile and in a typical way in these regions in both genes. Hence, the green sample corresponds to a high level of network interaction co-ordinatedness, as measured by the DNA methylation network interaction measure, $\rho_{XY} = 1$. The variation in the other regions of these genes do not well-explain each other, and so the red sample, which varies by a large amount in these other regions and varies less and in an atypical way in regions (a)–(d), corresponds to a low level of network interaction co-ordinatedness, $\rho_{XY} = 0.07$. Genes X and Y are likely to have different numbers of methylation measurement locations (i.e., variables X and Y are of different dimension). The ordering of the measurement locations has no influence on the calculation of ρ , as long as the ordering is consistent across samples.

A DNA Methylation Network Interaction Measure, and Detection of Network Oncomarkers

Thomas E. Bartlett^{1,3*}, Sofia C. Olhede^{2,3}, Alexey Zaikin¹

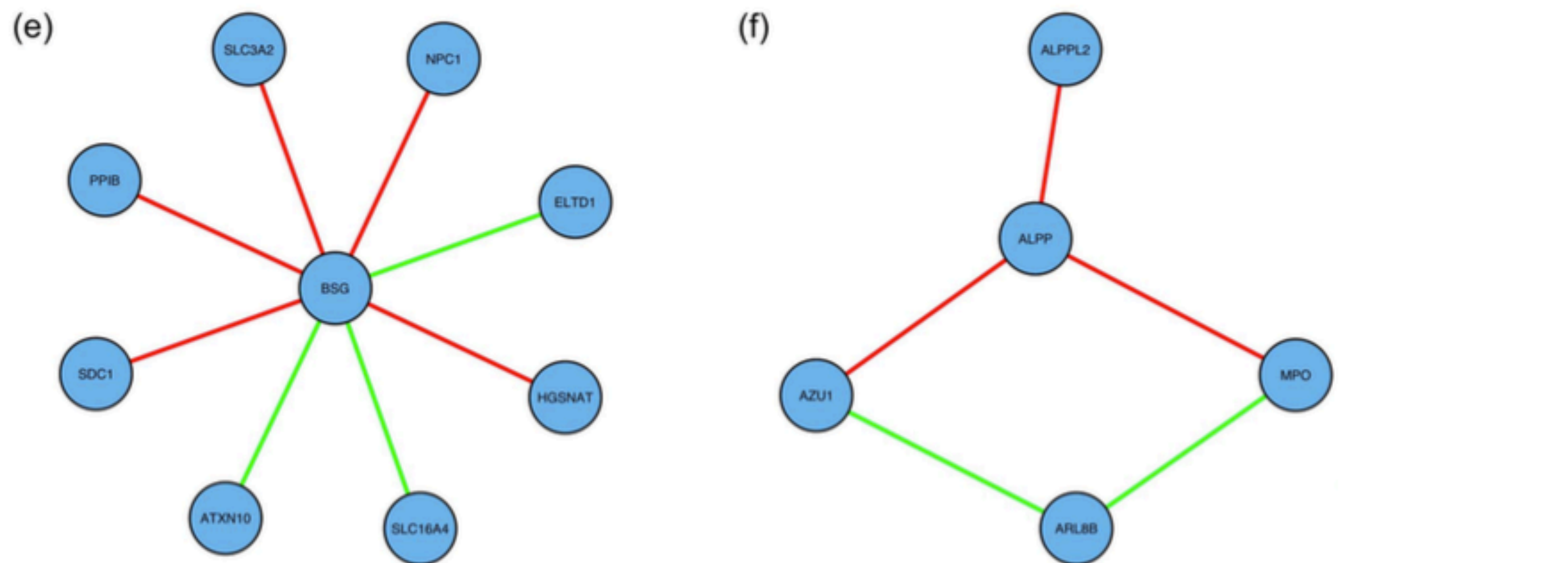


Figure 3. Smaller significant network modules: network diagrams. Network edges displayed in green and red indicate positive and negative hazard ratios, respectively, for the DNAm network correlation measure corresponding to that interaction; these correspond, respectively, to an

A DNA Methylation Network Interaction Measure, and Detection of Network Oncomarkers

Thomas E. Bartlett^{1,3*}, Sofia C. Olhede^{2,3}, Alexey Zaikin¹

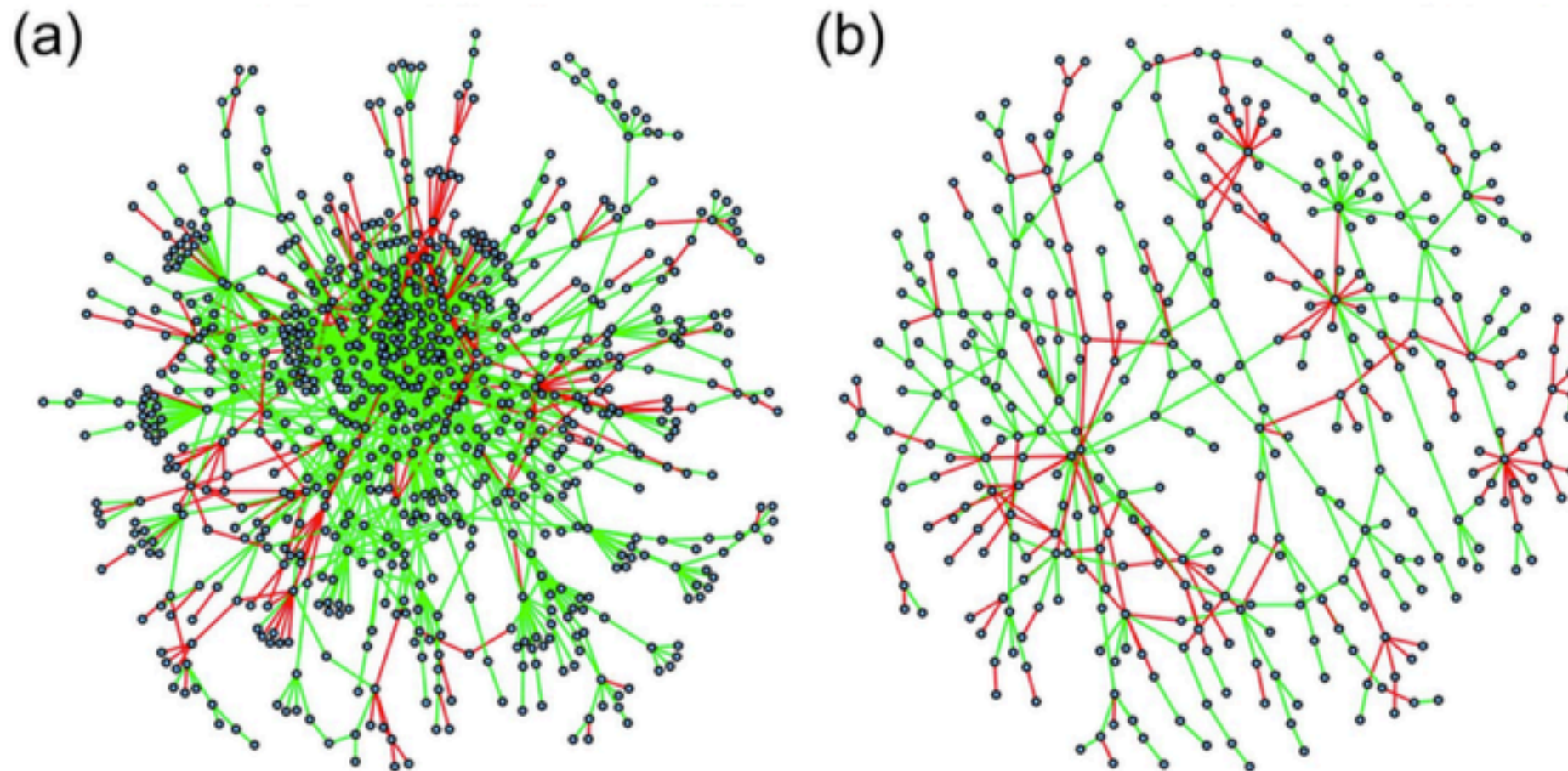
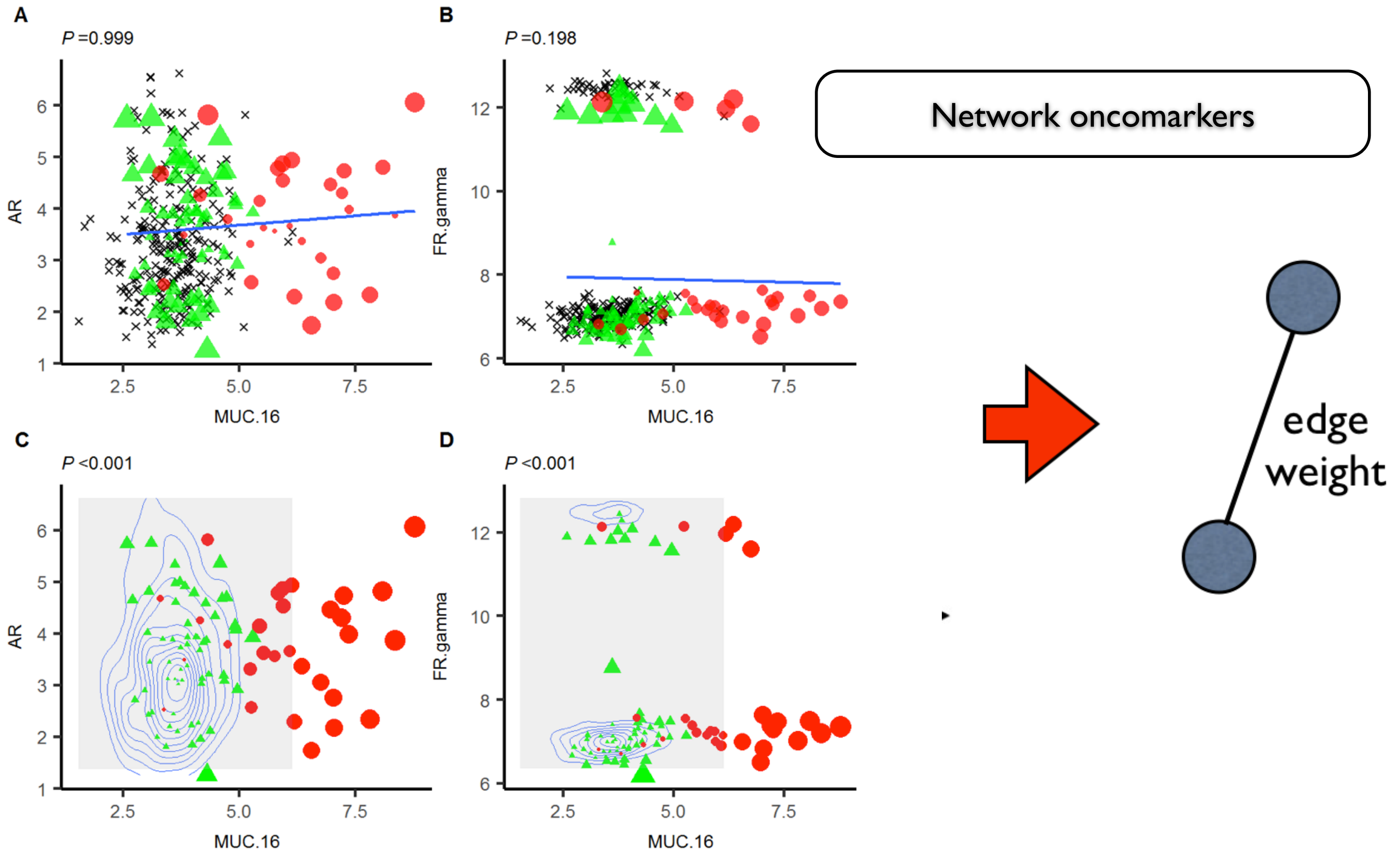


Figure 4. Larger significant subnetworks: network diagrams. Network edges displayed in green and red indicate positive and negative hazard ratios, respectively, for the DNAm network correlation measure corresponding to that interaction; these correspond, respectively, to an increase and decrease in 'network interaction co-ordinatedness' for worse disease prognosis. (a) the KIRC large subnetwork. (b) the LUAD large subnetwork. Further details about the corresponding network nodes (genes) for the top 5% of the degree distribution and top 25 significantly enriched gene sets appear in tables S5–6.

How to build a network if links are unknown?

Parenclitic networks for predicting ovarian cancer

Harry J. Whitwell¹, Oleg Blyuss², Usha Menon³, John F. Timms³ and Alexey Zaikin^{3,4}



RESEARCH ARTICLE

Parenclitic Network Analysis of Methylation Data for Cancer Identification

Alexander Karsakov¹, Thomas Bartlett², Artem Ryblov¹, Iosif Meyerov³, Mikhail Ivanchenko¹, Alexey Zaikin^{1,2*}

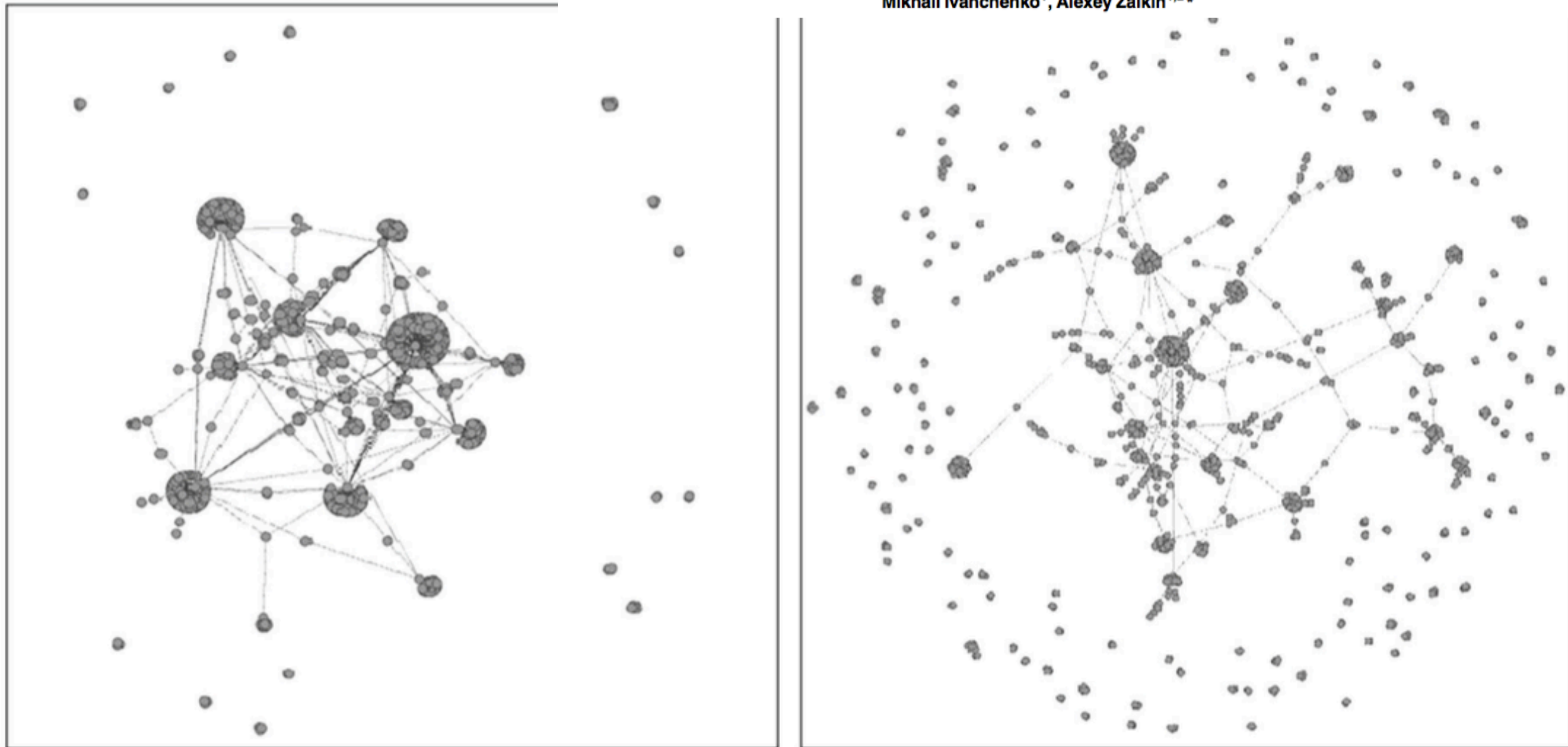
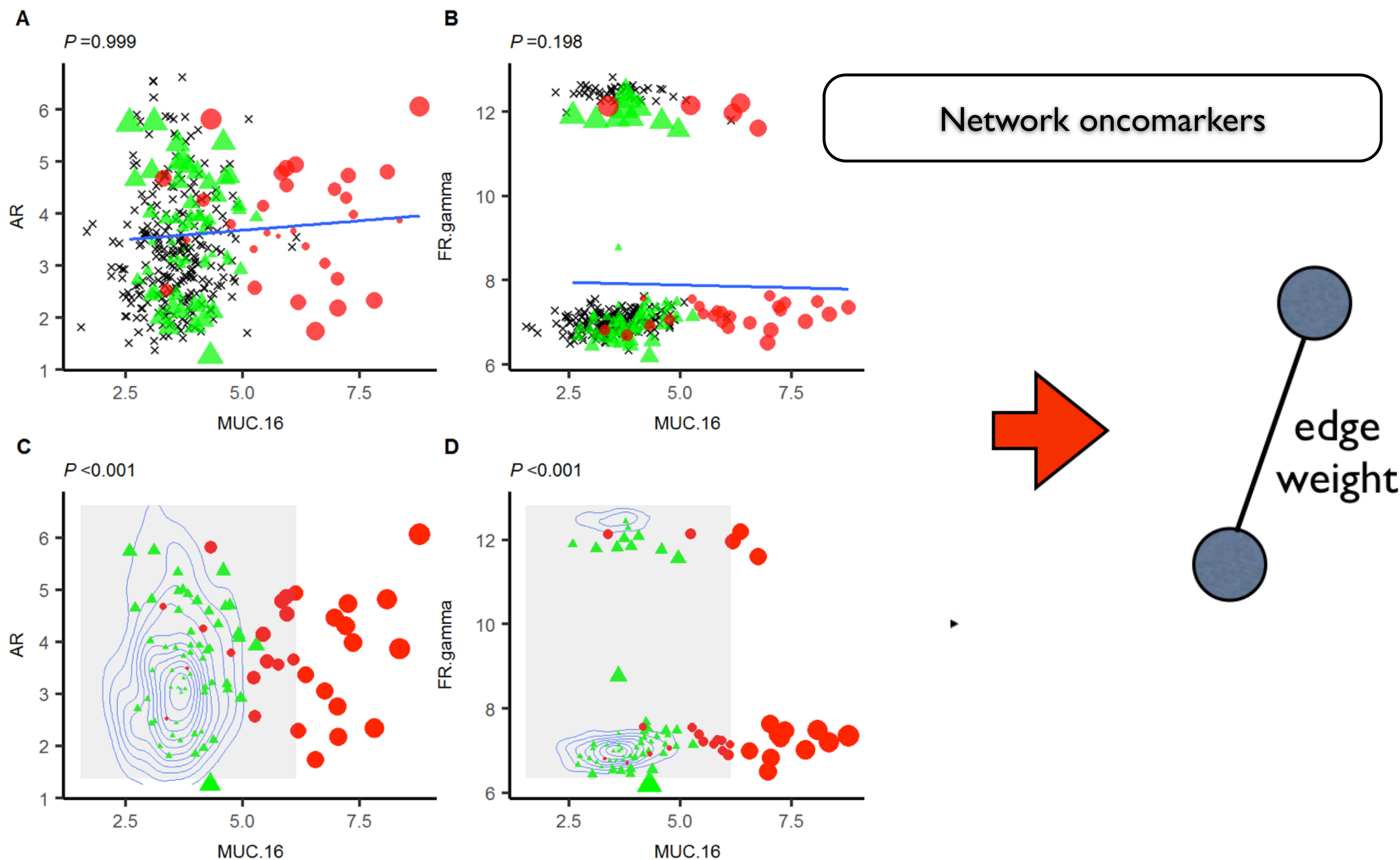


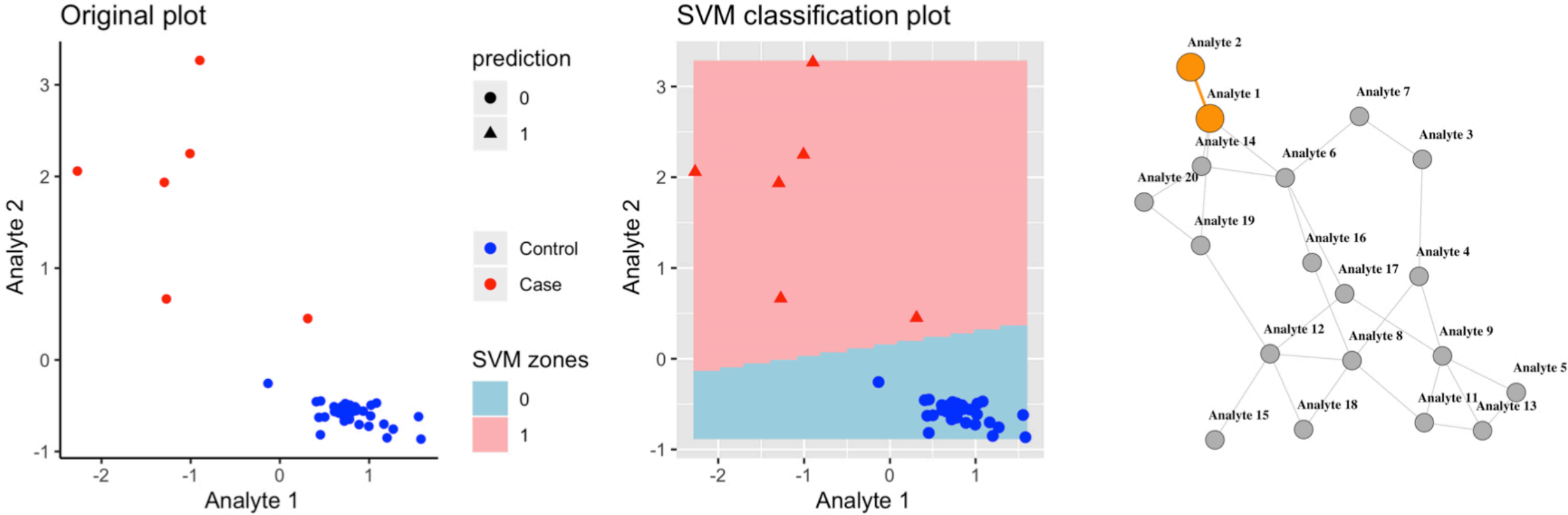
Fig 3. Typical examples of parenclitic networks constructed from gene methylation profiles for cancer (left) and normal (right) samples from BRCA data. Only a 1000 of the strongest edges and their incident nodes are shown. Note the pronounced modular structure for the cancer network.

Parenclitic networks for predicting ovarian cancer

Harry J. Whitwell¹, Oleg Blyuss², Usha Menon³, John F. Timms³ and Alexey Zaikin^{3,4}

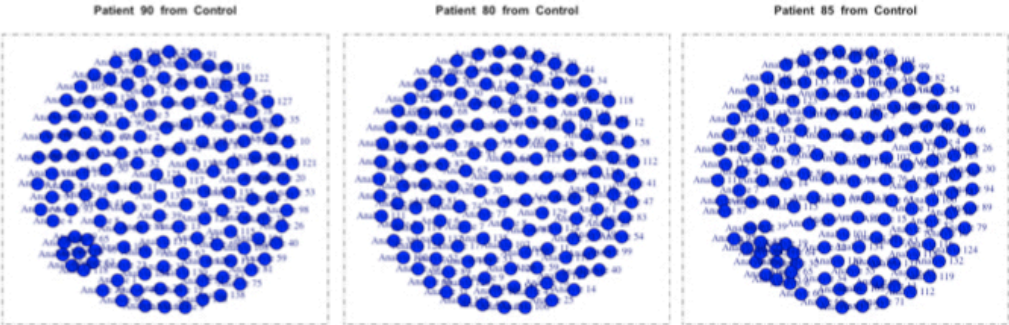


Parentclitic Network Construction (SVM approach as an example)

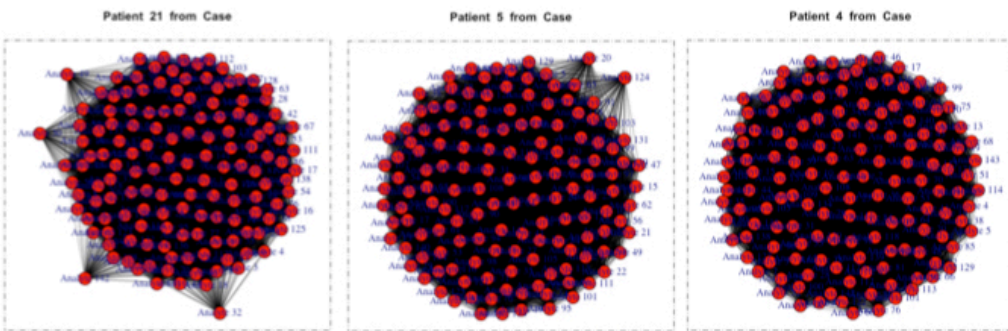


Network graph

Examples of Controls

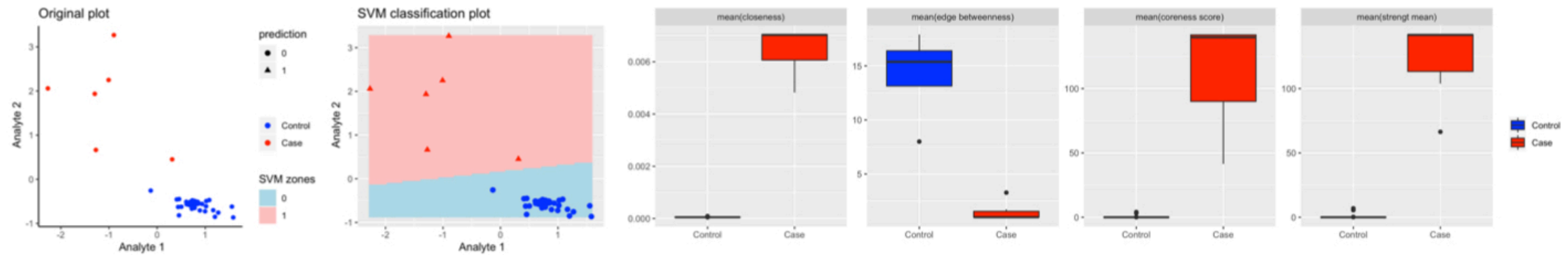


Examples of Cases

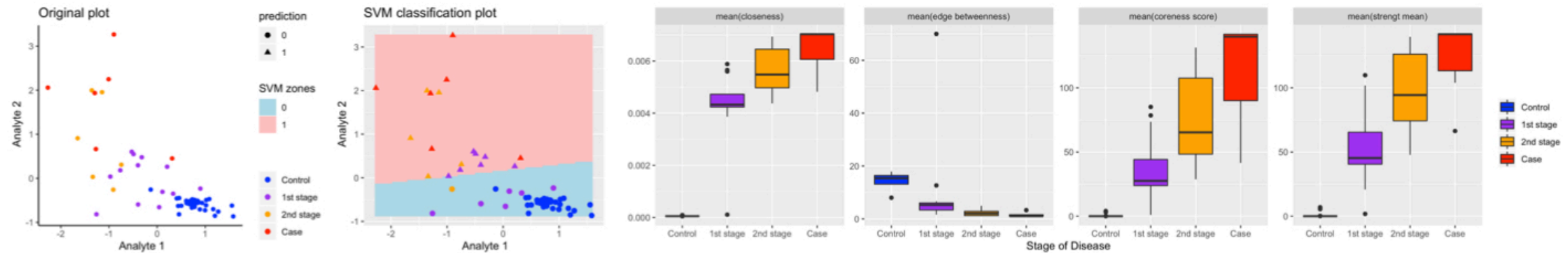


Examples of problems that can be solved using networks characteristics

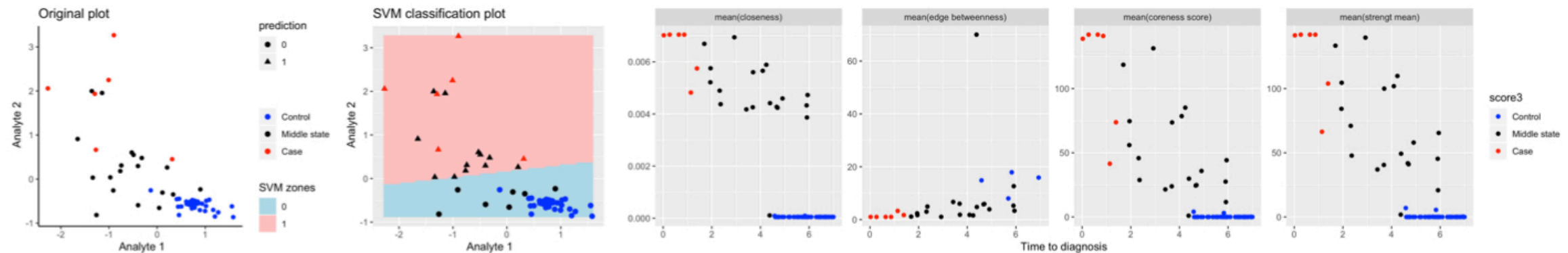
- **Case/Control** Classification (e.g. Disease/Health)



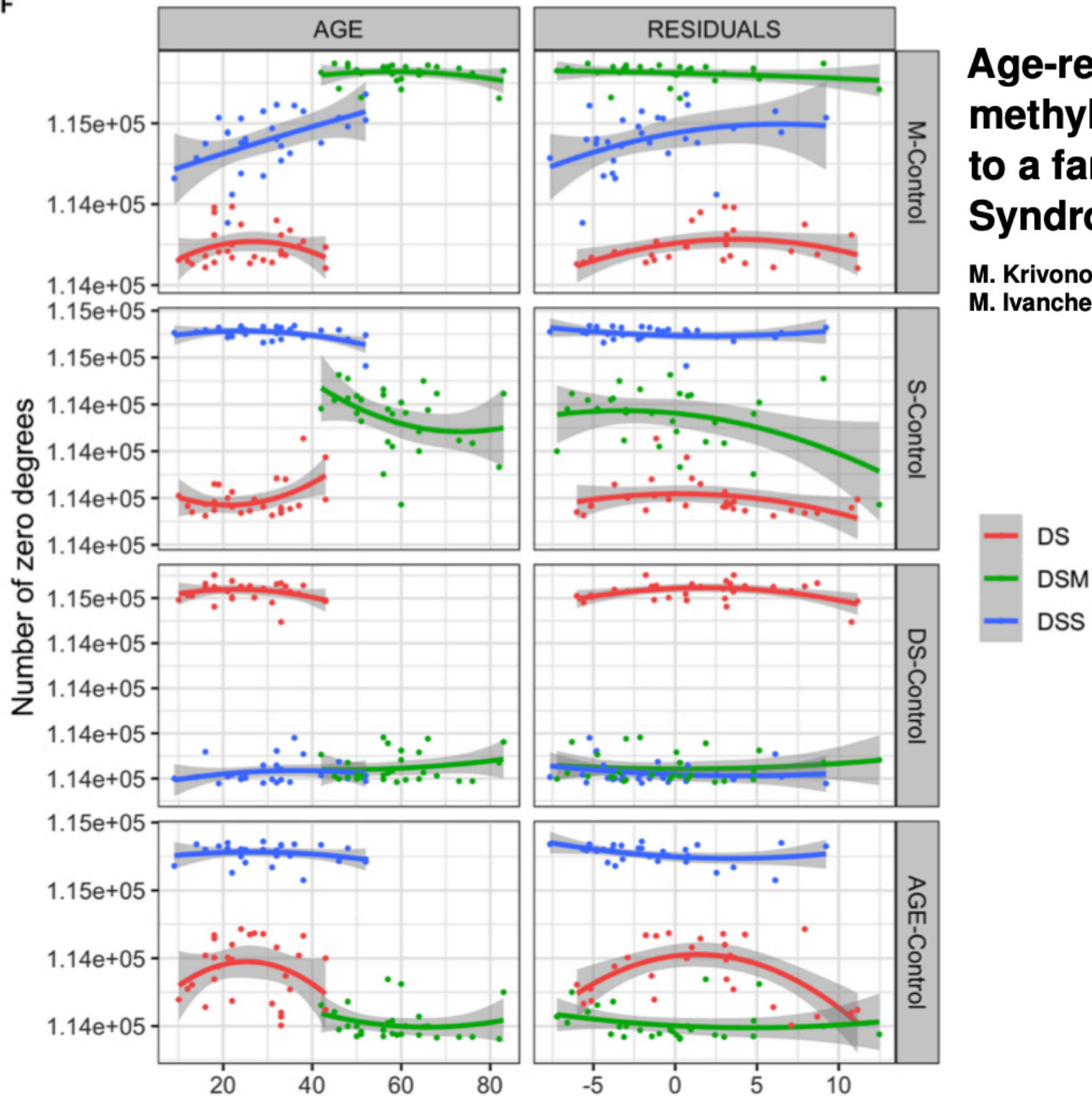
- Detection of *discrete state between Case and Control* (e.g. Stage of Disease)



- Detection of *continuous state between Case and Control* (e.g. time to Diagnosis)



F



Age-related changes in the network topology of DNA methylation probes: a parenclitic network approach to a family-based cohort of patients with Down Syndrome

M. Krivonosov¹, T. Nazarenko^{2,*}, M.G. Bacalini³, C. Franceschi^{1,3}, A. Zaikin^{1,2,4}, and M. Ivanchenko¹

1. **M-Control Network** — DSM group is *Control* group, DS group is *Case* group, DSS group is *Test* group;
2. **S-Control Network** — DSS group is *Control* group, DS group is *Case* group, DSM group is *Test* group;
3. **AGE-Control Network** — DSS group is *Control* group, DSM group is *Case* group, DS group is *Test* group;
4. **DS-Control Network** — DS group is *Control* group, DSS and DSM groups are *Case* group.



Dynamic predictive model for baseline early detection and follow- up re-evaluation of the risk of prostate cancer progression on active surveillance (PROGRESS Prostate)

Prostate cancer (PCa) is the second commonest male cancer worldwide, with 43% of patients being offered active surveillance (AS) as an alternative to radical treatment. However, a five-year dropout rate of 44% with pathological upgrading of 27% of re-biopsied cases within the first year of AS highlight the lack of robust risk-stratification models enabling both early detection and continuous re-evaluation of individualised progressive potential of PCa. With this in mind, here we present a CRUK ACED collaboration that seeks to develop a personalised dynamic predictive model able to estimate the risk of PCa progression throughout the whole AS continuum starting from the initial appointment. To develop the model, we will use a range of novel high-performance modelling methodologies utilising serial biomarker measurements, which we have previously developed and trialed as part of UKCTOCS trial.

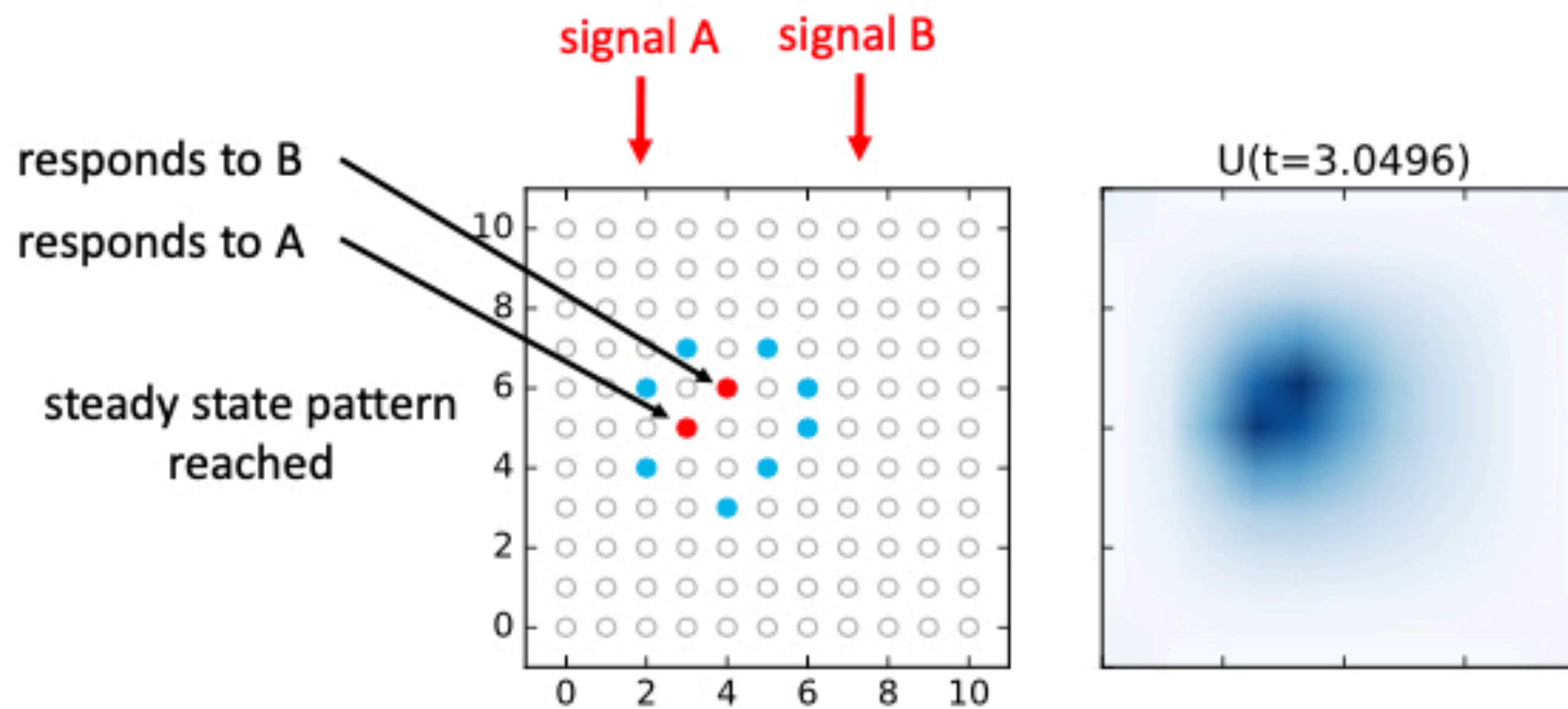
Deep Learning with Recurrent Artificial Neural Networks. We have recently shown that one of the most widely used deep learning techniques, recurrent neural networks (RNN), is capable of predicting the risk of developing ovarian cancer based on measurements of serial CA125. (26) To use RNN as part of this project, we have developed a neural network architecture based on state- of-the-art AI findings and using Long Short Term Memory RNNs, especially RNNs with Gated Recurrent Unit, and shown further improvement of cancer early detection (unpublished data). In the current project, we will further adapt this architecture for a further improvement of a risk- stratification model, potentially integrating findings from the MMT and BCP approaches with the RNN.

Genetic intelligence (student project)

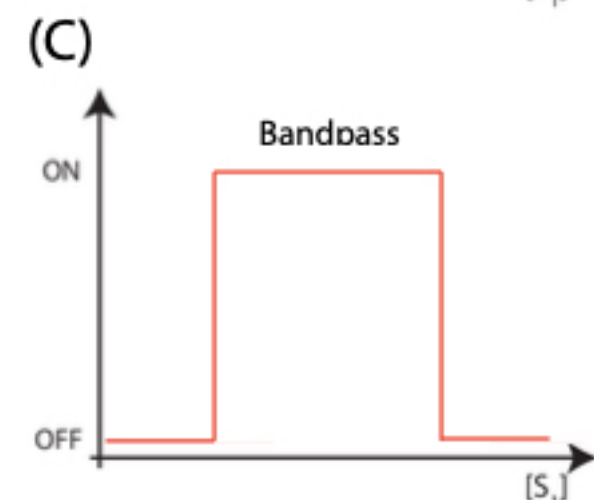
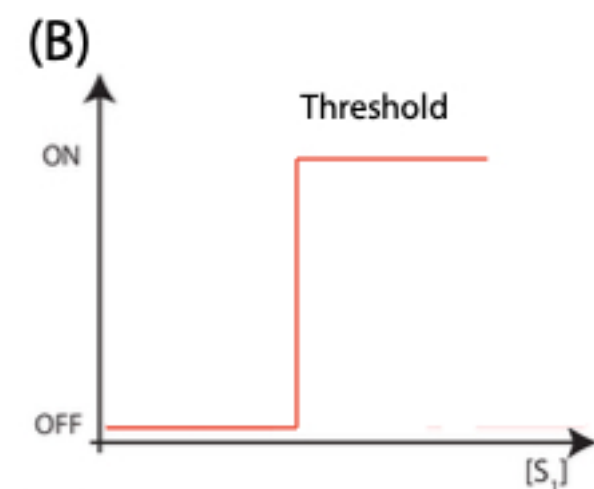
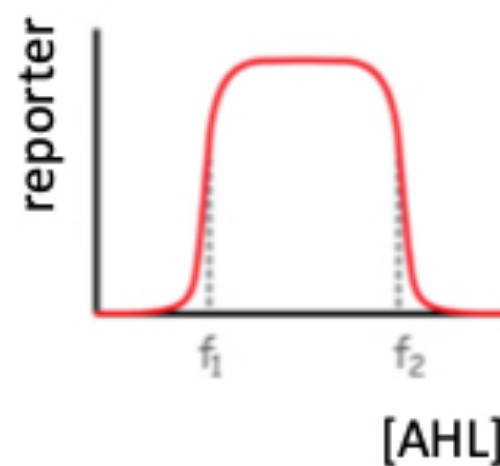
Building biological computers from bacterial populations



Neythen Treloar
Supervisor: Chris Barnes



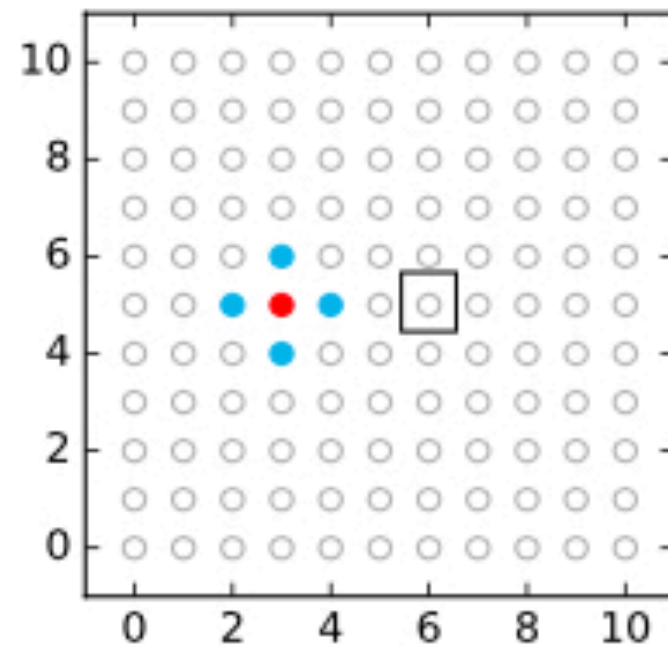
receiver colonies
contain a band detector
that responds to AHL and
switches on/off



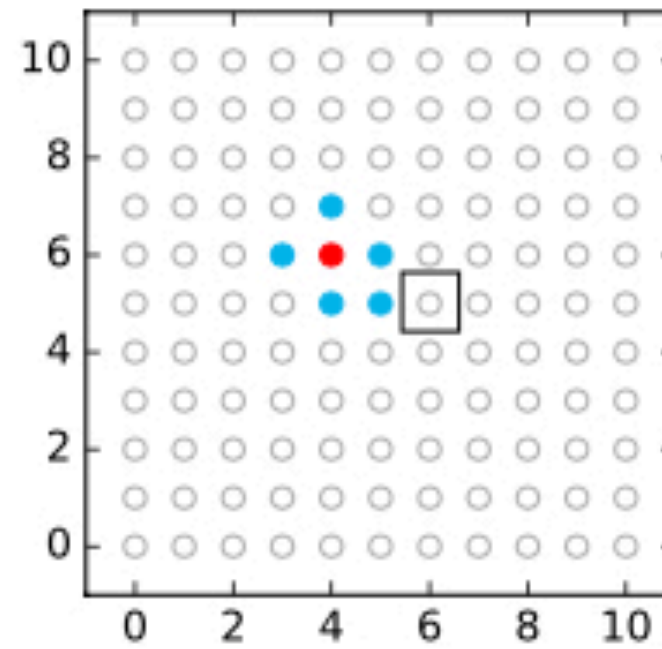
Main idea:

Spatial pattern can be used for signal integration and computation

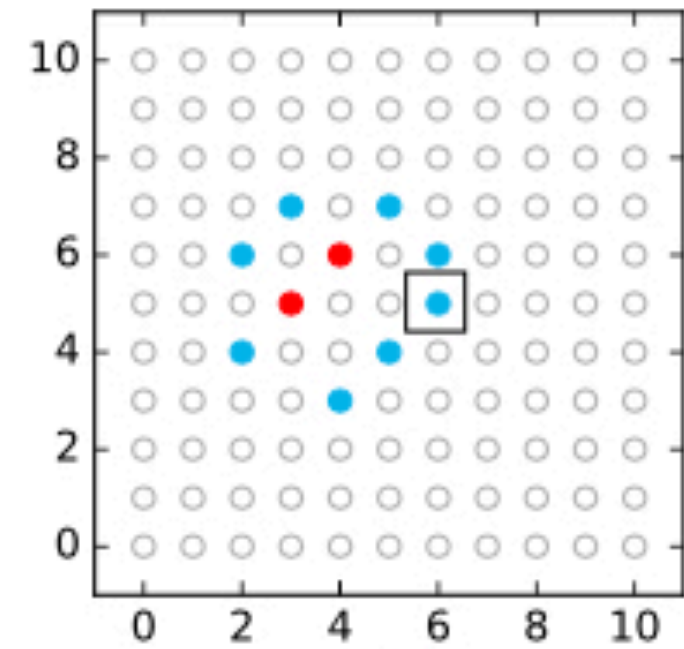
B on, A off



B off, A on



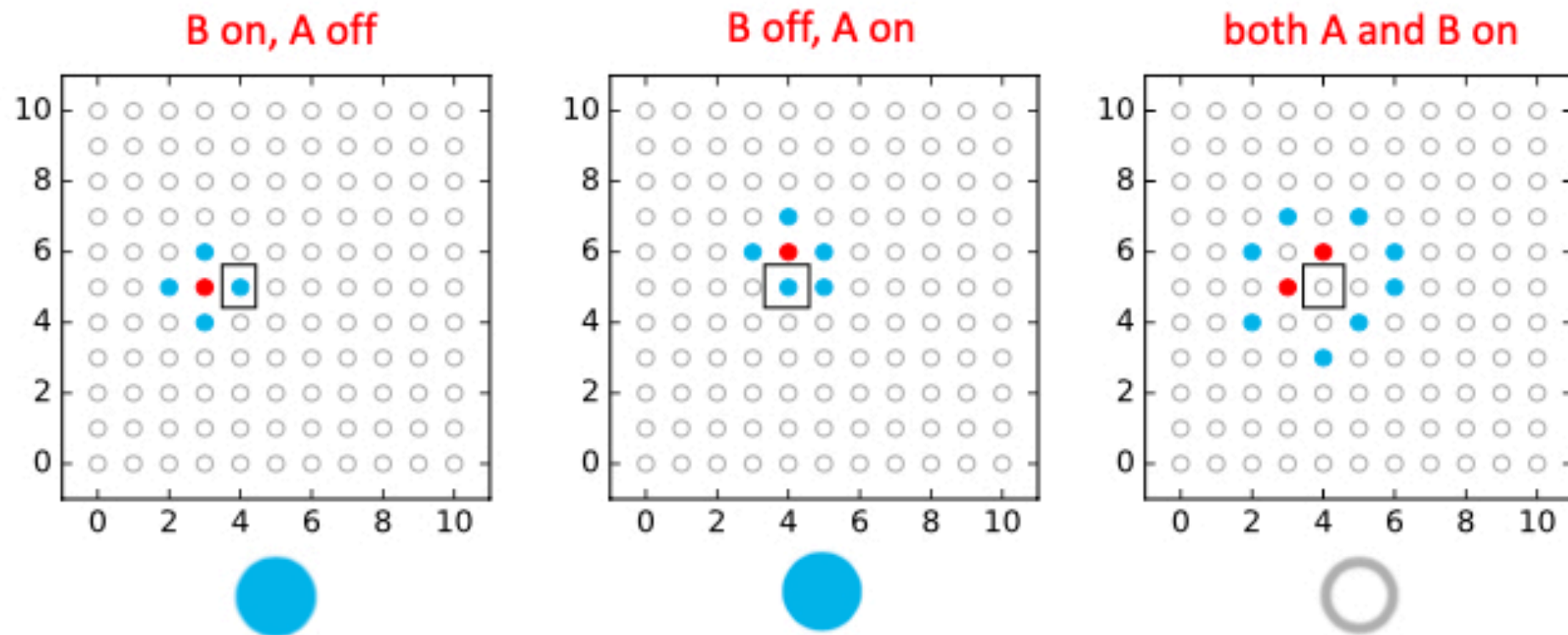
both A and B on



A	B	AND
0	0	0
0	1	0
1	0	0
1	1	1

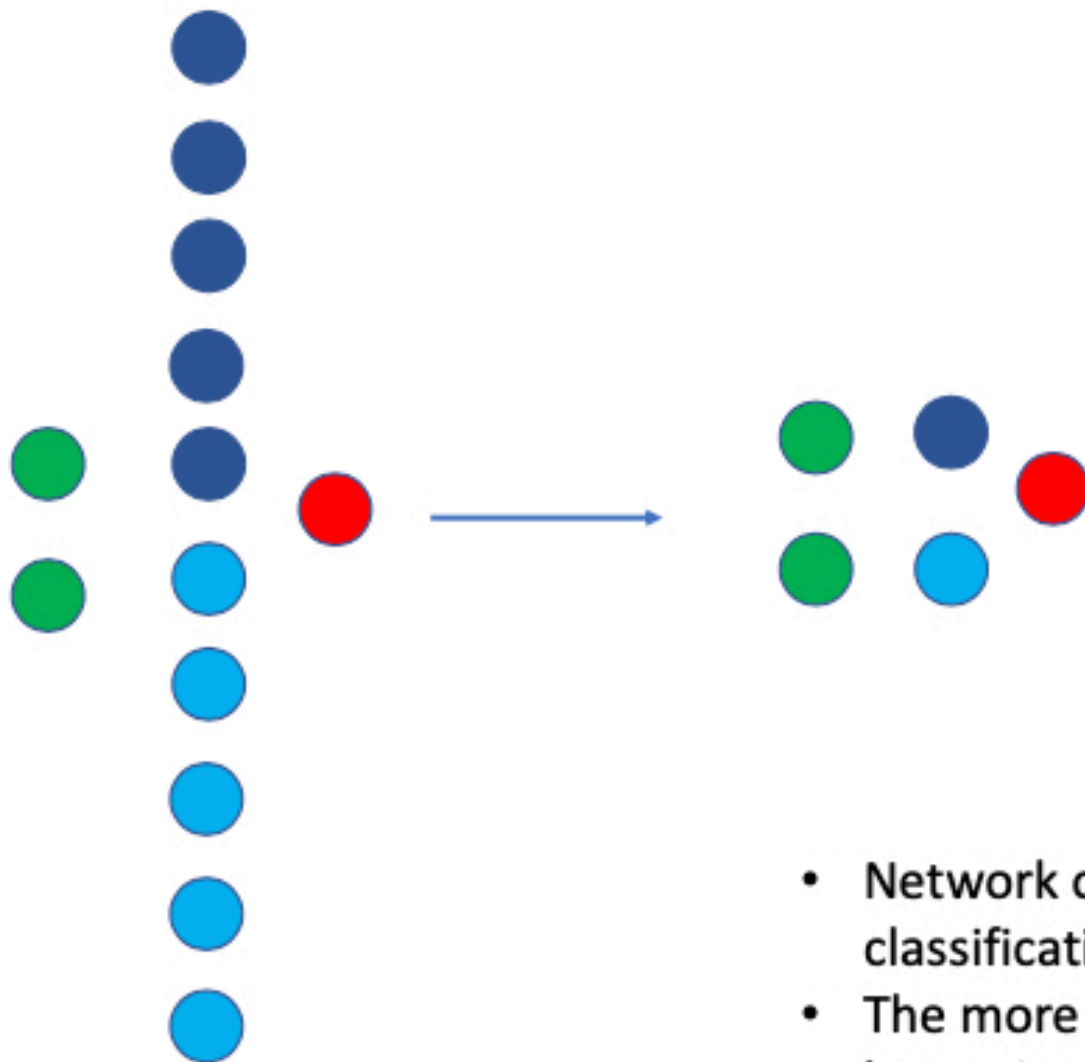
Main idea:

Spatial pattern can be used for signal integration and computation

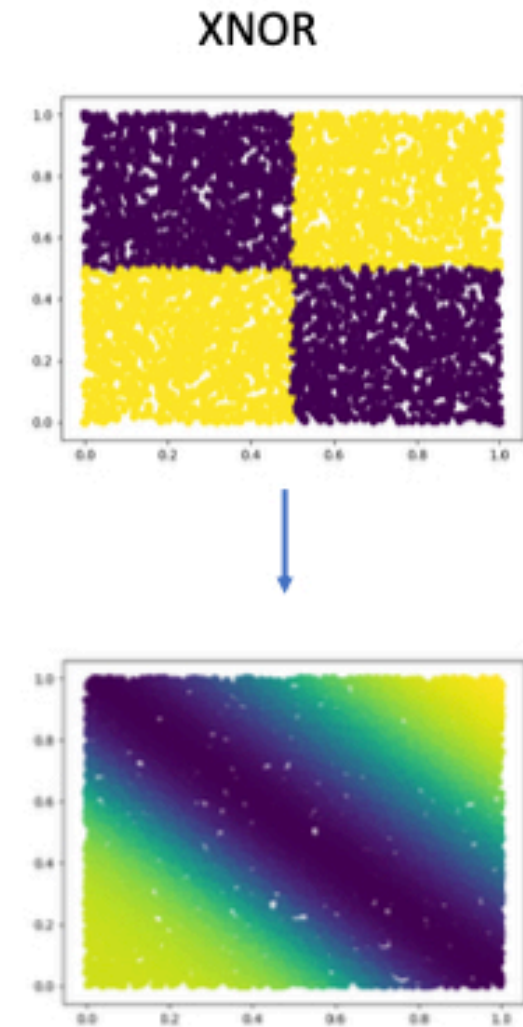


A	B	XOR
0	0	0
0	1	1
1	0	1
1	1	0

Network trained with these constraints using regularization to encourage sparsity.

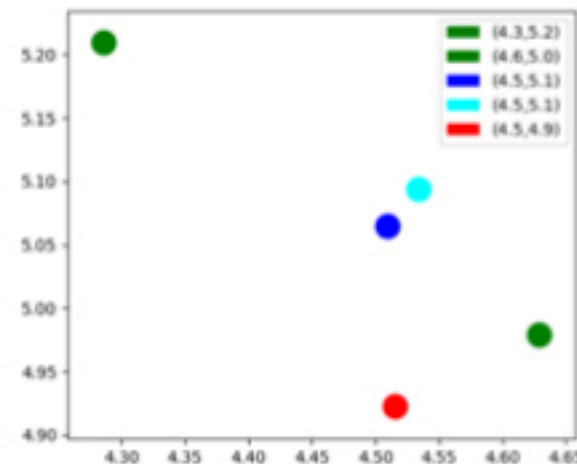
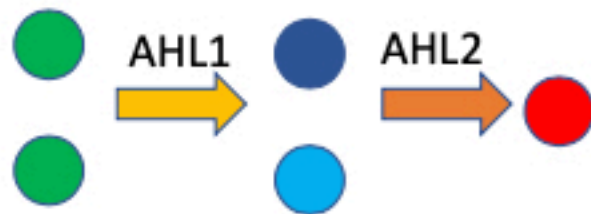


- Network output: enough for digital classification
- The more constraints we can overcome the better it will perform



Weights extracted from trained network and evolutionary algorithm used to find node position

- This assumes we have two AHLs



Target:

[[3.6815872, 3.7029088],
[6.8024187, 6.783618]]

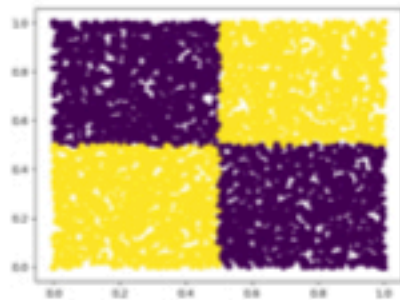
[7.0231166, 5.7998238]

Solution:

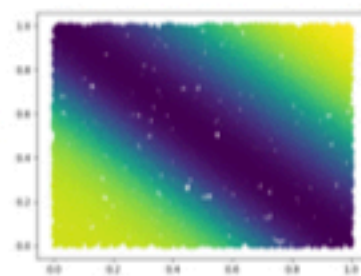
[[3.6642652], [3.6659336],
[6.80611], [6.792463]]

[7.0273304], [5.795528]

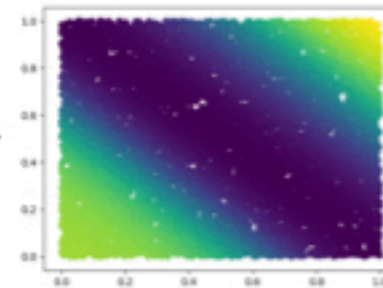
XNOR



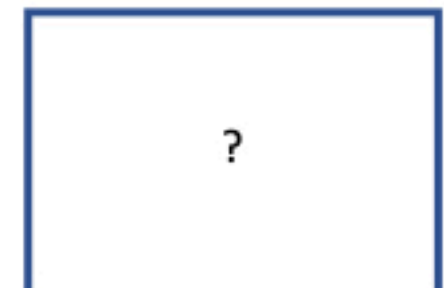
Network trained
with constraints



Weights recalculated
from positions



Diffusion system



Main open question:
longitudinal data analysis of multiplex
networks with different space and time scales

